TEL AVIV UNIVERSITY
The Iby and Aladar Fleischman Faculty of Engineering
The Zandman-Slaner School of Graduate Studies

Shape change algorithm for a tensegrity device

A thesis submitted toward the degree of
Master of Science in Mechanical Engineering

by
Avner Bronfeld

February 2010

TEL AVIV UNIVERSITY
The Iby and Aladar Fleischman Faculty of Engineering
The Zandman-Slaner School of Graduate Studies

Shape change algorithm for a tensegrity device

A thesis submitted toward the degree of
Master of Science in Mechanical Engineering

by
Avner Bronfeld

This research was carried out in the Department of Solid Mechanics, Materials and

Systems under the supervision of

Dr. Uri Ben-Hanan

Dr. Offer Shai

February   2010

Acknowledgments

First of all for their help with this study, I would like to thank the members of the research team:

Uri Ben-Hanan
Leon Ginzburg
Efim Mohr
Offer Shai
Michael Slavutin
Itay Tehori

Last but not least, I wish to thank my parents, without whom none of this would have been possible.

Avner Bronfeld.

Abstract

Tensegrity devices are special truss-like structures composed of struts in compression and cables in tension. In order to keep a tensegrity device rigid, its members must be pre-stressed. By using actuators to vary the lengths of the struts and cables a tensegrity devices can reconfigure its geometry i.e., change its shape. This ability makes tensegrity devices suited for applications such as self deploying structures, smart structures and even robots.

Two key steps in the reconfiguration of tensegrity devices are form-finding, the process of identifying the geometries in which all the device's members are stressed known as its singular configurations, and shape change, the process of moving the device from one singular configuration to another without loosing its stiffness.
Current known shape change methods rely heavily on time and processing power costly methods, like simulations and large scale optimizations, for these steps.

This work presents a new shape change control strategy which is based on the special properties of Assur Trusses. The concept of Assur Trusses (also known as Assur Graphs), long known in the field of kinematics, has recently been reformulated by mathematicians from rigidity theory community, and new theorems and algorithms have been developed. The control strategy developed during the research is fast and does not require a lot of processing power. This strategy is applicable to any device whose topology is an Assur Graph, of which there is an infinite number.

The proposed shape change algorithm allows the device to move from one singular position to another while maintaining its stiffness at all times. The shape change is accomplished by changing the length of the device's actuated members.

With this algorithm some of the controlled members change their lengths in some arbitrary fashion to reach the desired shape, while only one member is controlled in such way that will maintain the device's stiffness.

The strategy has been developed and tested on a prototype tensegrity device that was designed and built for practical experiments. Experiments with the prototype device showed that the new strategy does enable the device to change its shape.

Table of contents

1 Introduction

1.1 Tensegrity

The word Tensegrity is an abbreviation for Tensile Integrity which was coined by Buckminster Fuller (Fuller, 1962).

There are many different definitions to the word, but they all describe a system that contains two types of elements in equilibrium; tensile elements which resist tension forces and compressive elements that resist compression forces.

The "classic" engineering Tensegrity system is a truss-like structure that is composed of struts or bars in compression and cables under tension, fig. 1.1 a.

However there are many other types of Tensegrity systems, for example a balloon in which the rubber skin is the tensile element and the gas inside is the compressive element, fig. 1.1 b. Another example is the bodies many living organisms, in which the bones are the compressive elements while the muscle and tendon fibers are the tensile elements, fig. 1.1 c.

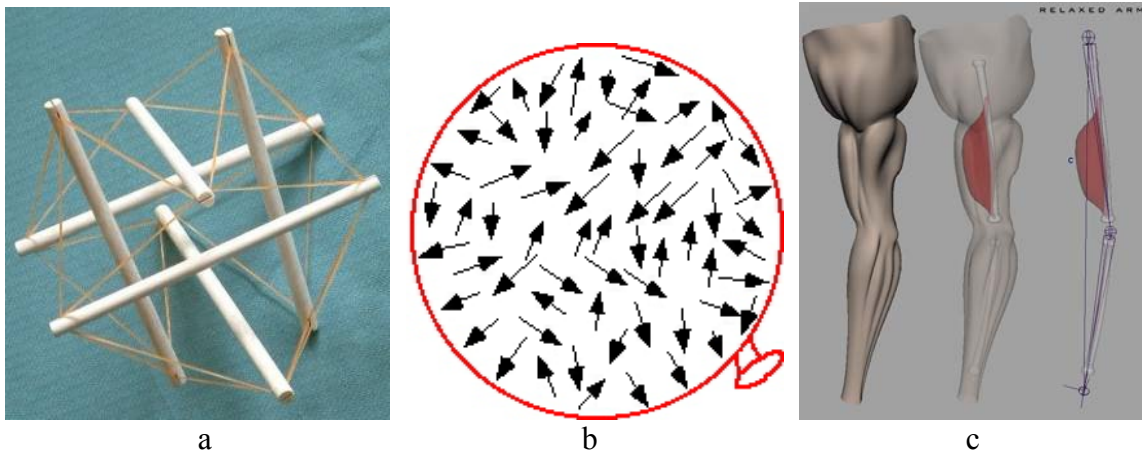a   b   c

Figure 1.1 - Tensegrity systems, (a) structure (b) balloon (c) human arm.

In order to keep a Tensegrity structure rigid, its members must be pre-loaded.

An important feature of the "classic" Tensegrity structure is that its elements are only loaded axially and only in one direction. Although the global structure may bend under an external load, none of its elements is loaded with a bending moment. Furthermore, each member is always subjected only to either tension or compression but never to both, therefore the tension members can be wires or cables instead of rods.

There are several advantages to members that are cables or wires over members that are rods. They can be designed more efficiently because they are not subjected to buckling. They can be rolled to a length much shorter than their extended length for storage. They provide opportunities for actuation and sensing (Sultan et al., 2000; Skelton et al., 2001).

Because of these properties the Tensegrity principle can be used to design lightweight structures and shape changing structures.

1.2 Shape changing structures

There are several types of structures that have the ability to change their shape:

An active structure is defined by Soong and Manolis (Soong and Manolis 1987) as one consisting of two types of load-resisting members: the static or passive members, and the dynamic or active members.

A deployable structure is an assembly of prefabricated members or elements that can be transformed from a compact or folded configuration to a predetermined expanded form of a complete stable structure capable of supporting loads.
A structure with an inverse transformation is called a collapsible or foldable structure. The functionality and the feasibility of the design of such structures depend not only on the structural behavior of the expanded configuration under service loads but also on the structural response during deployment and during dismantling. The multiple design criteria during deployment and during dismantling as well as in the deployed configuration make these structures very different from conventional structures (Gantes, 2001).

Self deploying structures are active deployable structures in which actuation of the active members allows the structure to transform into its expanded form under its own power.

A smart structure is a structure that is capable of sensing and reacting to its environment in a predictable and desired manner, through the integration of actuators and sensors. In addition to carrying mechanical loads, smart structures may alleviate vibration, automatically perform precision alignments, or change their mechanical properties or shape on command (Parker, 1994).

When a structure has the ability to change shape involving large displacements it can be described as a mechanism or a robot.

Tensegrity devices must maintain forces in their members at all times to prevent collapse. Tensegrity devices also have the property that actuation at one location can translate into movement at multiple locations, and conversely, movement at one location can be caused by multiple actuators. Due to this property, multiple control strategies may exist for a single behavior (Paul et al., 2005b).
Because of that developing a control strategy for tensegrity devices is usually more complex than for conventional devices. This work will focus on a new type of control strategy for a tensegrity shape changing device.

The process of developing a tensegrity shape changing device can be divided into four stages:
- Selecting the type of the device (its topology).

6

- Selecting two or more shapes for the device (geometries).
- Developing a method to transform the device from one shape to the other.
- Building and activating the device.

The following sections will give an overview on each of these subjects.

1.3 Types of tensegrity structures

Tensegrity structures can be categorized in several different ways.

One categorization is referred to as the class number, defined by Skelton, as appears in (Skelton et al., 2001):

A class k tensegrity structure is a stable equilibrium of axially loaded elements, with a maximum of k compressive members connected at the node(s).

A class 1 tensegrity structure has only one compression member terminating at each node, class 2 can have 2 etc.

A common approach is the categorization of tensegrity structures based on the number and type of members in the structure, usually categorization is by the number of rigid bars in the structure.
The naming convention is a capital T followed by the number of rigid bars (T-3, T-4 etc).
The rigid bars in a tensegrity structure can be connected in many different ways. The different possible topologies fit into families of tensegrity structures.
One of the most studied tensegrity families is called the prism family, the basic structure of which consists of two equal end polygons in parallel planes joined by members at their vertices. The end polygons are not required to remain of equal size or in parallel planes and may even become skew, but they must be geometrically similar (fig. 1.2).
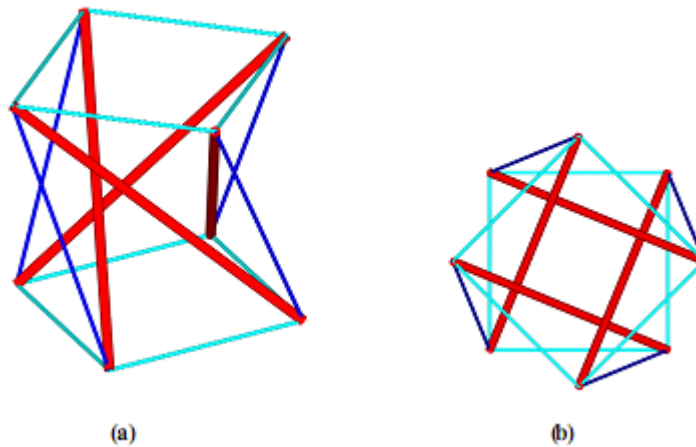

(a)   (b)

Figure 1.2 - a T-4 tensegrity prism, (a) perspective view (b) top view

Another family of tensegrity structures is based on polyhedra formed from all triangular faces with a mobility of zero. They include the tetrahedron, octahedron, decahedron, dodecahedron, and icosahedron (Fig 1.3.).
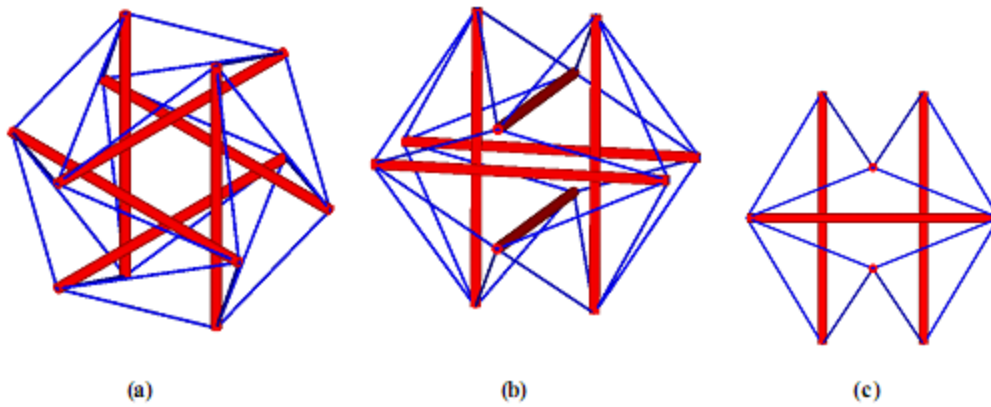
Figure 1.3 - a T-6 tensegrity Icosahedron, (a) top view (b) perspective view (c) side view

Two or more tensegrity structures may be combined to create more complex structures, the original structures do not have to be identical, but for pacrical purposes they usually are (fig 1.4).
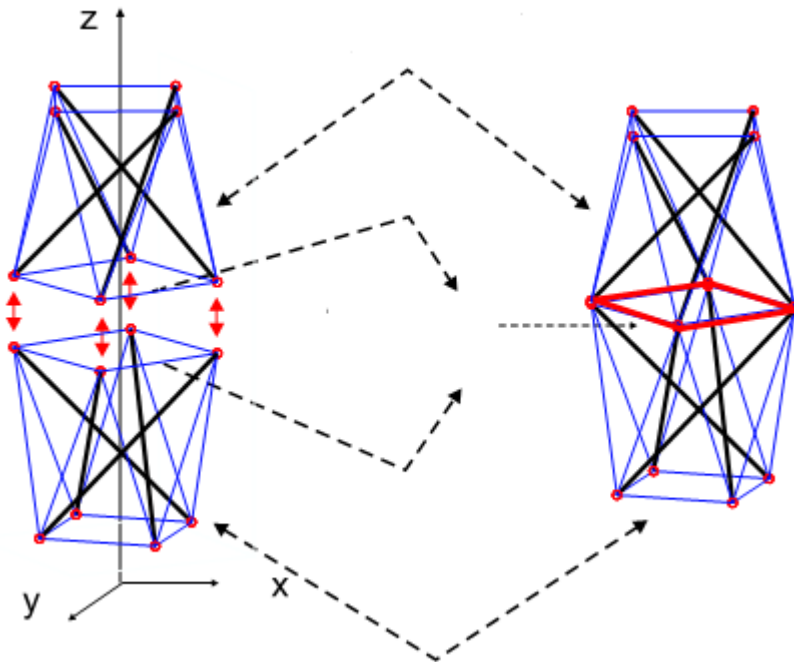

Figure 1.4 - Two class1 T-4 tensegrity prisms combined into a class 2 tensegrity tower.

The device studied in this work is based on a class one, T-3, tensegrity prism (where the end polygons are triangles) (fig 1.5).
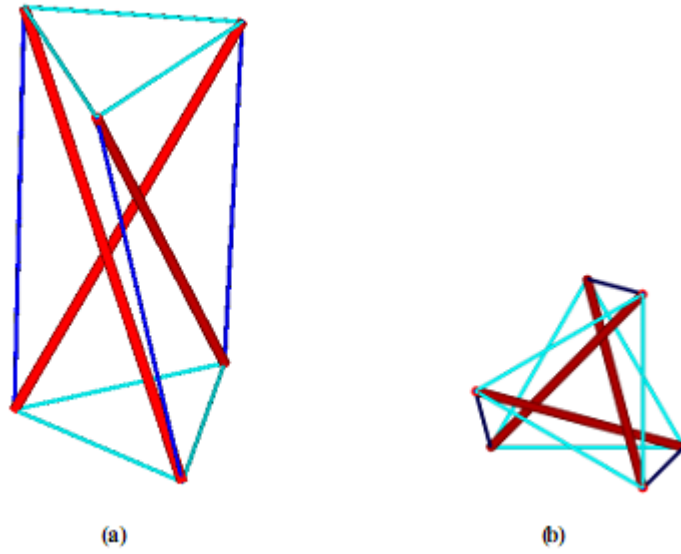
Figure 1.5 - a T-3 tensegrity prism, (a) perspective view (b) top view

1.4 Form finding

After the topology of the device has been selected, its geometry must be decided. Unlike trusses, merely examining the topology of a tensegrity structure cannot be used to determine whether it is rigid or not. Even if the structure topology is suitable for a tensegrity structure, it will be rigid only in specific geometries which are called singular configurations. For a shape changing device, at least two geometries are needed, a starting geometry and a final geometry, for example, a folded geometry and a deployed geometry. Form finding is the process of locating a rigid geometry for a tensegrity structure.

1.4.1 Singular configurations

A large number of trusses and mechanisms can move into special positions where they become Tensegrity structures. These positions correspond to specific link lengths of the system members that place the device in a singular position. Only in these specific singular positions would the structure not collapse if specified rigid links were replaced with flexible tension members. These tensegrity configurations allow the system to be pre-stressed, which is required to give a tensegrity system its stiffness.
In order for a tensegrity structure or device to maintain its rigidity, its geometry must correspond to a singular configuration. If the device must move between singular positions while supporting any weight, resisting any external forces or simply retaining its shape, it must also be in singular positions at all times between the starting and ending position.
It is easy to see that finding these singular positions, commonly referred to as the form finding problem, is one of the main issues in any work relating to tensegrity.

1.4.2 Methods of finding tensegrity structures' singular configurations

C. Sultan developed a method of identifying singular configurations by checking "prestresbility conditions"; a set of nonlinear equations and inequalities.
In order to derive the general prestressability conditions they applied the principle of virtual work (Sultan et al., 2001):

Assuming E tendons and N degrees of freedom, the total virtual work W is given by:

$$W = \sum_{j=1}^{E} W_j = \sum_{j=1}^{E} T_j \sum_{i=1}^{N} \frac{\partial l_j}{\partial q_i} \delta q_i = \sum_{i=1}^{N} \delta q_i \sum_{j=1}^{E} \frac{\partial l_j}{\partial q_i} T_j = \delta q^T A(q) T.$$

where
T   is the vector of tendon tensions
l   is the vector of tendon lengths
q   is the vector of generalized coordinates (state variables)
δq   is the vector of virtual displacement of the generalized coordinates

The elements of the matrix A(q), called the equilibrium matrix, are given by

$$A_{ij} = \frac{\partial l_j}{\partial q_i}, \quad i = 1,\ldots,N, \quad j = 1,\ldots,E.$$

Since the virtual work must be zero for every virtual displacement δq, there must be

$$A(q)T = 0$$

Since at a prestresable configuration all tendons must be strictly in tension, that is, T_j must be positive for every j, the prestressability conditions are

A(q)T = 0 and $T_j > 0$ for j = 1,…, E

A necessary condition for T to have positive elements is that the kernel of A(q) is nonzero. In terms of A(q) this condition gives rise to the following:

$$\det(A(q)) = 0 \quad \text{if } N = E,$$

$$\det(A^T(q)A(q)) = 0 \quad \text{if } N > E.$$

If N<E the kernel of A(q) is guaranteed to be nonzero.
Solving the general prestressability conditions is difficult. Previous research has focused on numerical solutions. Sultan presented several Tensegrity structures for which the prestressability conditions can be analytically solved for certain configurations.

W. Whittier developed a form finding method based on finding the "boundary of non-assembly" (Whittier, 2002). The method is based on the fact that in any structure or mechanism a set of link lengths can be found that does not allow the system to be assembled. Bar systems can also be constructed of link lengths such that they exist on the boundary of non-assembly. An example of this is shown in figure 1.6.

(a)   (b)   (c)
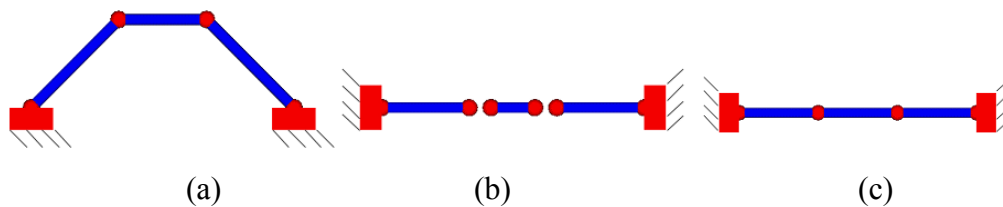
Figure 1.6. Four bar mechanism with different bar lengths.

In mechanism (a) it is obvious that the chosen set of link lengths allows assembly. The links of mechanism (b) on the other hand have been chosen such that they cannot be assembled. Mechanism (c) has been built so that it is on the edge of being able to be assembled, on the boundary of non-assembly.
Stable positions for Tensegrity structures lie on the boundary of non-assembly. Mechanism (c)'s ground link can be replaced with a strut and the other links with cables and the mechanism would become a Tensegrity structure.

This same principle is also valid for three-dimensional structures and mechanisms.

The ideal method for finding Tensegrity positions for a given topology would be to find and define the whole region of non-assembly for the topology. Completely defining the region of non-assembly is difficult for the complex three-dimensional tensegrity structures, however, it is easier to find specific positions on the boundary of non-assembly.

The following algorithm for finding tensegrity positions has been implemented in a MATLAB program. The program starts with a set of members connected in truss form that may or may not be in a Tensegrity position. A numerical root finding method is used to find the position of the truss that satisfies the kinematic constraints for each link.

Using numerical methods, moving the structure into the Tensegrity position is attempted by adjusting the length of one chosen link.

If the structure starts in a truss position in which assembly is possible, then the chosen link will be changed in length (tension member shortened or compression member lengthened) to move the structure towards the boundary of non-assembly. The chosen link is adjusted in length until the closure equations (kinematic constraints) begin to become unsolvable. This shows that the structure is on the boundary of a non-assembly volume and has reached a prestressable configuration.

If the structure were to have started with link lengths such that assembly is not possible, the chosen link would be changed in length (tension member lengthened or compression member shortened) to move back towards an assembly region until all constraint equations just began to be met. This would also cause the structure to be on the boundary of non-assembly.

To verify that the truss is indeed in a Tensegrity position, a check is performed using static force analysis.

Using this approach, the Tensegrity position corresponding to the given set of link lengths can always be found. At this point, a new set of link lengths (all but one) can be chosen to make a new structure, and the process can be repeated to find the corresponding Tensegrity position.

In this work the approach to form finding was similar to Whittier's (Whittier, 2002) in that it also starts with an arbitrary geometry and then one link length is changed in length until a singular position is reached. The difference was that instead of using a program to numerically solve the problem for a model, the actual link length in the prototype device was changed until the device became pre-stressed, at which point the link's length is measured by a sensor instead of needing to be calculated.
The approach developed in this study does not require the formulating and solving of static or kinematic equations.

Williamson (Williamson et al., 2003) characterized the singular configurations of tensegrity structures as configuration where all string elements are in tension, all bar elements are in compression and all nodes are in a state of static equilibria (with or without external forces).

The authors used vectors to describe the structure's elements and the forces in it, eliminating the need to use direction cosines and the subsequent non-linear functions that follow their use. They used matrices to describe the relations between the elements. By enlarging the vector space in which they characterized the problem, the mathematical structure of the equations allowed treatment by linear algebra methods. This reduced the form finding problem to a series of linear algebra problems.

Another approach for finding singular configurations being developed by our team is based on the connection between tensegrity, trusses and mechanisms.

Any truss which is under a unique self stress can be turned into a tensegrity by replacing the bars under tension with cables and bars in compression with struts. A similar process can be used on mechanisms which are in dead-end positions.

Therefore any method developed in the fields of structures and mechanisms to find self stressed configurations or dead-end positions may also be applied for finding tensegrity singular positions.

For example, figure 1.7 shows a truss and a tensegrity device which share the same topology (known as "triad") and geometry.
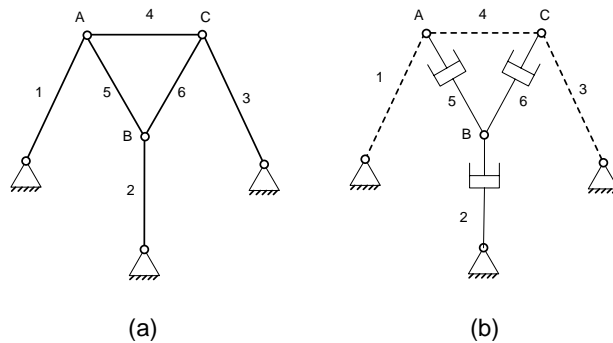

(a)   (b)

Figure 1.7 - A truss (a) and tensegrity device (b) with identical topology and geometry.

There are several ways to characterize the singular position. For above topology all singular positions occur when the continuation of lines 1, 2 and 3 intersect at a single point (fig 1.8.) (Shai and Polansky, 2006). Using this geometrical constraint, a closed analytical definition of the singular position of the tensegrity device can be defined.

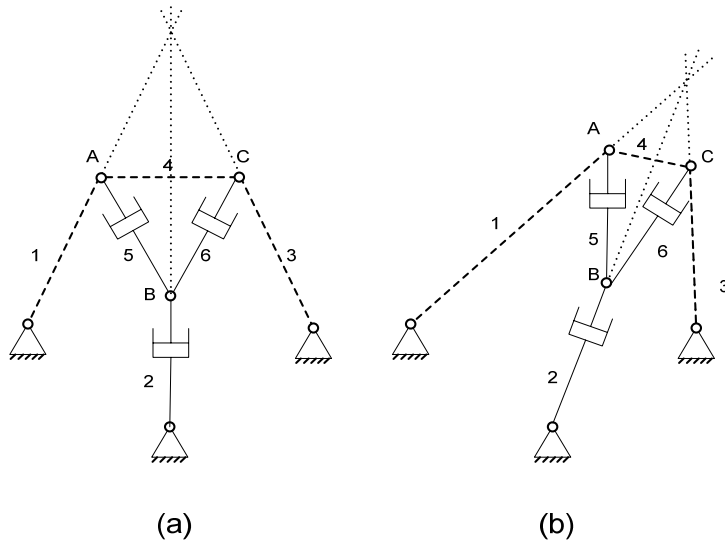(a)   (b)

Figure 1.8 - (a,b) sample singular configurations.

Ben-Horin and Shoham (2006) analyzed the singularity in a class of Gough–Stewart platform mechanisms. The topology of one member of this class matched the topology of the T-3 tensegrity prism (fig. 1.9).
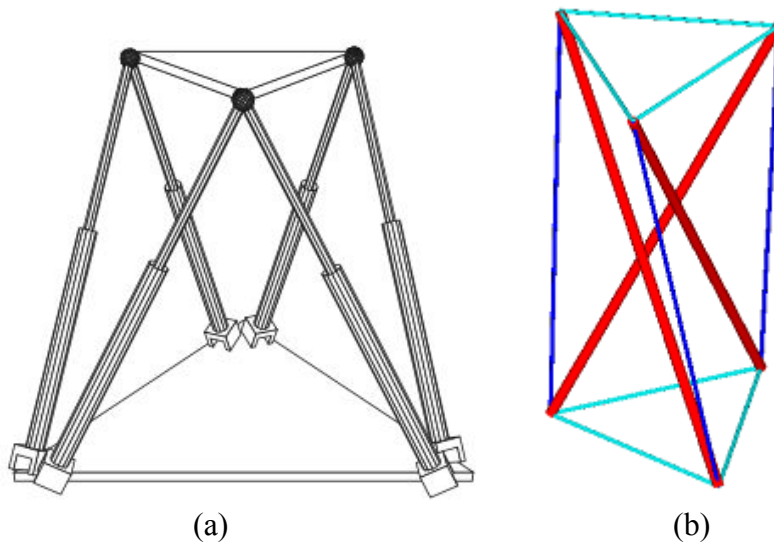

(a)   (b)

Figure 1.9 - (a) Stewart platform (b) T-3 tensegrity prizm

They discovered that for this class the singular configurations occur precisely when four planes, defined by the positions of the joints, are concurrent in a point.
Using this geometrical constraint, a closed formula analytical definition of the singular position of the T-3 tensegrity prism has been defined.

1.5 Shape change

Shape change is a process in which by adjusting the lengths of some of a tensegrity device's members, the geometry of the device is altered, usually for the purpose of changing its position and orientation along a prescribed path while maintaining its stiffness.

Kanchanasaratool and Williamson (2002) studied two path tracking algorithms; a quasi-static algorithm based on an open loop piecewise constant input, and a gain scheduling algorithm based on an interpolation of "locally designed" controllers.

The authors used a system of nonlinear differential equations where u is the control input, z is the state of the device and y is the performance output.

$$\dot{z} = f(z;u)$$
$$y = h(z)$$
(1.5.1)

In general, given the tracking time T and the initial state $z(0)$, a finite time path tracking problem can be formulated as an approximate "inverse problem" in which the control signal $u(t)$ is to be computed from the given trajectory $y(t)$ so as to minimize the integral of the tracking error.
As a result of the nonlinear nature of the model, no solution to this problem is available, and so instead, the authors divided the trajectory into R segments with endpoints $y_1..y_R$, and seek a sequence of inputs $u_1..u_R$ such that y_i is an equilibrium condition for each given u_i.

If there exists an invertible function H such that $y_i = H(u_i)$ than a suboptimal tracking solution is given from the inverse function

$$u_i = H^{-1}(y_i)$$
(1.5.2)

However, even if an inverse were known to exist, an explicit form would be unlikely. Based on the assumption that an inverse exists, the authors used an artificial neural network approximation to H^{-1}. As is well-known, a neural network must be "trained" using a data obtained from input-output data of the steady state system.
The training data consisted of 1456 pairs of steady state input-output data obtained from simulations for various bar lengths.

Various simulations were then performed with different values for R and T and the following observations were made:
For a constant time increment Δt, tracking performance improves as R increases.
For a constant number of increments R, tracking performance improves as Δt increases.
For a constant number of tracking time T, tracking performance improves as R increases (Δt decreases).

The tracking performance significantly deteriorated for T < 50 seconds, and the inability to further reduce the tracking time is consistent with the open loop nature of this quasi-static approach to tracking. To overcome this problem the authors used a "gain scheduling" control algorithm. This algorithm divided the shape change process into a constant number of operating points and for each point sought a nonlinear feedback controller whose gains were determined from the linearized model of the system at the operating point. Between the operating points the controllers used gains that were interpolations of the gains at the operating points.

Sultan and Skelton (2003) presented a shape change strategy based on the existence of a set of equilibrium configurations. In the state space this set is represented by an equilibrium manifold. For this strategy the equilibrium manifold to which the initial equilibrium configuration and final equilibrium configuration belong must first be identified.

This strategy is best suited to symmetrical deployment of tensegrity devices, since the symmetrical parametrization limits the dimension of the manifold. Figure 1.10 graphically illustrates the equilibrium manifold of a 6 bar tensegrity device. The device has 6 actuators but it needs only 3 parameters to describe its position because of the symmetry requirement.

Due to the small number of parameters, the allowable configurations of the tensegrity structure can be conveniently visualized as an equilibrium surface plotted in the three dimensions of the parameters. Each dot on the graph represents an allowable equilibrium (singular) configuration that has been identified and the black line represents the desired shape change path. Without the symmetry requirement the device will need at least 6 parameters to describe it position which would require a six dimensional manifold which would be much harder to generate.
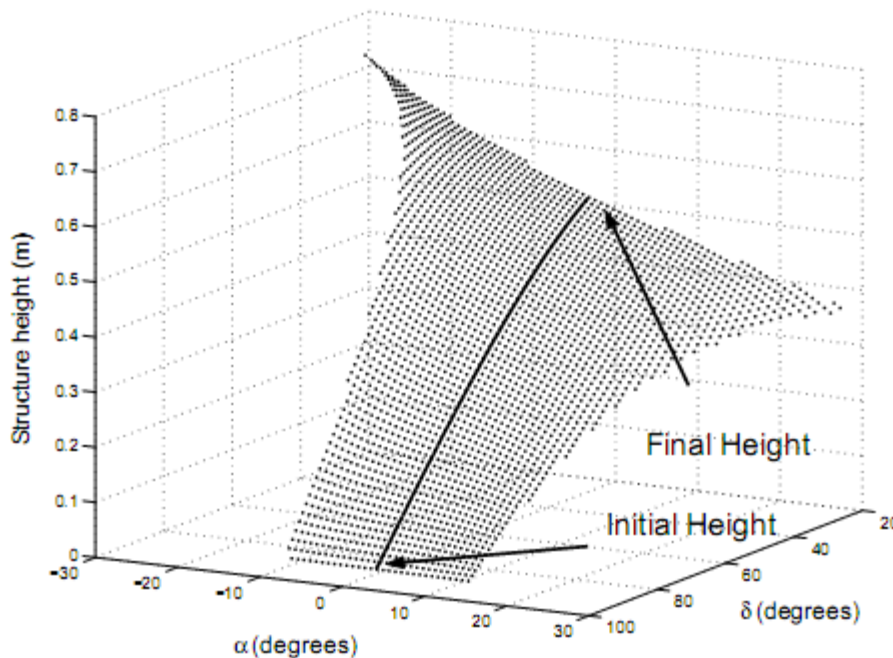

Figure 1.10 - Graphic illustration of a 3 dimensional equilibrium manifold.

17

The main idea is to conduct the deployment such that the deployment path is close enough to this manifold. The advantage in doing so is that, due to the proximity of the deployment path to this manifold, the successive configurations the structure passes through are not much different from the equilibrium ones. If these equilibrium configurations have certain properties (for example, all tendons are in tension and sufficient clearance between the isolated rigid bodies exists), then the deployment can be conducted slowly enough such that the intermediate configurations the structure passes through posses the same properties.

One way to ensure that the deployment path is close to the equilibrium manifold is by letting the control variables take values only in the set of the equilibrium manifold controls. That is to say the controls are allowed to take only values corresponding to equilibria which belong to the equilibrium manifold. If the change in control variables is smooth enough, then the system undergoes slow motions, remaining close to this manifold.

Pinaud et al. (2003) used the above mentioned strategy for symmetrical deployment but observed that there is a rapid increase in the number of independent parameters when asymmetrical shapes are considered. For the six bar device mentioned above the number of parameters can be as high as 36, compared with 3 for the symmetrical deployment case. In cases when there are many independent parameters the equilibrium manifold becomes immensely large and a search to characterize this space would most likely be fruitless and yield no special insight.

The tendon trajectories for shape change of an asymmetric tensegrity device were computed using iterative nonlinear optimization programs which allowed for easy specification of constraints on the geometry of the device.

In this shape change method, the desired shape change is divided into n stages.

For each ith stage of the n stages, a non-linear optimization program is activated with inputted constraints which are based on the tensegrity equilibrium requirements and the desired trajectory of the device. The program returns a solution p_i which contains the geometrical properties of the device on the ith stage.

At the end of each optimization iteration, the solution p_i is used to compute the members' lengths and so construct the tendon length trajectory. In addition, the solution p_i is used as an initial guess to the solution p_{i+1} of the next iteration that follows. This ensures every solution is the closest solution to its two neighboring solutions.

After the n iterations have been run, the constructed member length trajectories become the open loop control laws that are used to change the shape of the device.

Van de Wijdeven and de Jager (2005) developed the following method for shape change. First a reference trajectory for the nodal positions of the tensegrity structure is found solving a series of optimization problems. Due to the number of nodes in a non-trivial structure, the optimization was a larger scale one. It was also non-convex and nonlinear. Due to the scale of the problem, no dynamics were included in the constraints. Dynamic effects were handled by a feedback controller.

To obtain an actual reference trajectory, the desired shape change and time span were divided into N sub-shape changes and time steps. At every time step on the total time span, the sub-shape change was optimized while the constraints were met. When all the N optimizations are feasible, they result in (sub-)optimal values for the design variables and a total shape change that was obtained by carrying out the sub-shape changes sequentially.

The reference signals contained only a limited number (N) of operating points on the trajectory. To generate data between two operating points, linear interpolation of the reference signals was applied. Note, however, that moving from one operating point to the next still led to discontinuous first derivatives due to the linearly interpolated reference trajectory. This resulted in excitation of the structure.

Depending on the material used for the tendons, a tensegrity structure can have little damping. When the reference trajectory is only used for feedforward control, this lack of damping can lead to poorly damped structural vibrations during and after the shape change. To reduce vibrations a feedback controller is introduced.
The linearly interpolated desired nodal positions and tendon forces are used as reference signals for the controller.

In the above mentioned methods the shape changing process is divided into many stages and for every stage a form finding must be performed. The method presented in this work requires form finding only twice, for the starting position and for the final position.

1.6 Experimental Devices

Despite the large body of theoretical work in the field of Tensegrity, only few smart Tensegrity devices that have actually been built are mentioned in the literature.

At University of California's Structural Systems and Control Lab Pinaud et al. (2003) experimented with the Tensegrity device shown in fig. 1.11
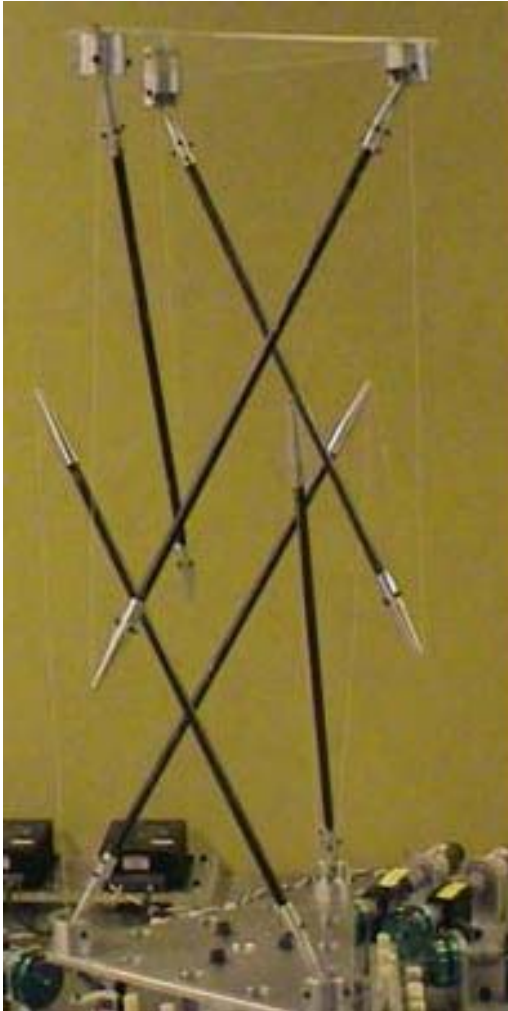

Fig 1.11 - Class 1 Tensegrity mast.

The device was a class 1 two stage mast, composed of two stages, each based on a T-3 prism. It was built to demonstrate the feasibility of a method to accomplish shape control of Tensegrity structures. The device utilized six D.C. motors as tendon actuators. Each of the six motors controlled one pair of identical tendons in the structure for a total of twelve actuated tendons (Fig 1.12).
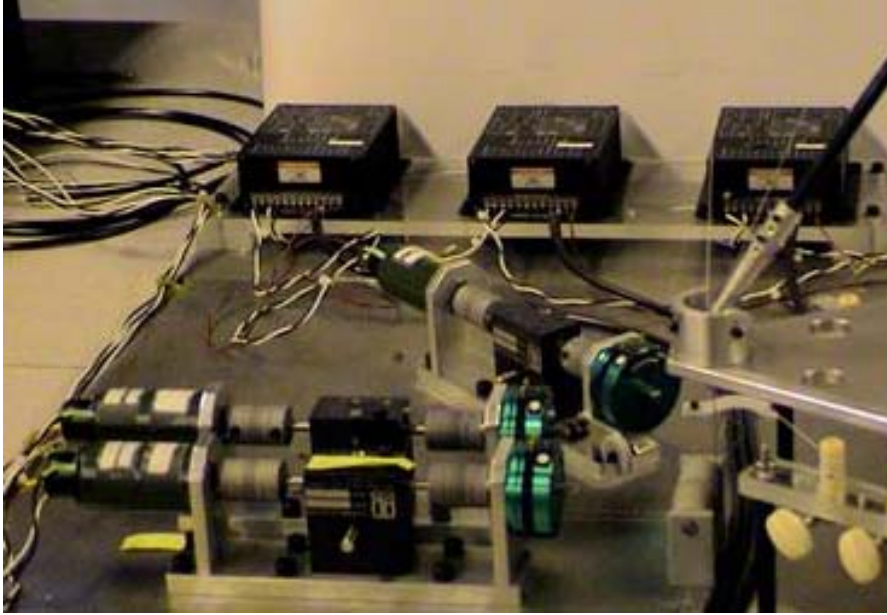
Figure 1.12 - Tendon actuation motors.

The tendon trajectories for reconfiguration of the tensegrity device were computed using iterative nonlinear optimization programs. The trajectory of the center of mass of the top plate was used to generate constraints for the geometry optimization process.

This method utilized the direct computation of the admissible static equilibrium configurations that are at the same time solutions to the inverse kinematic problem for the desired end-effector path.

The motion of the structure was assumed to be quasi-static so the dynamics of the reconfiguration could be ignored. An open loop control strategy based on slowly moving from one stable equilibrium state to another was used to track the trajectory. Stability along the deployment path was assured only if the movement was slow enough, unlike the prototype device presented in this work which maintains its stability over a wide range of speeds.

Another device studied by Pinaud et al. (2004) and by Masic and Skelton (2004) at CSSL is shown in fig. 1.13. The device was a class 2 mast composed of two stages, each based on a T-3 prism. The device was only capable of symmetric vertical deployment.
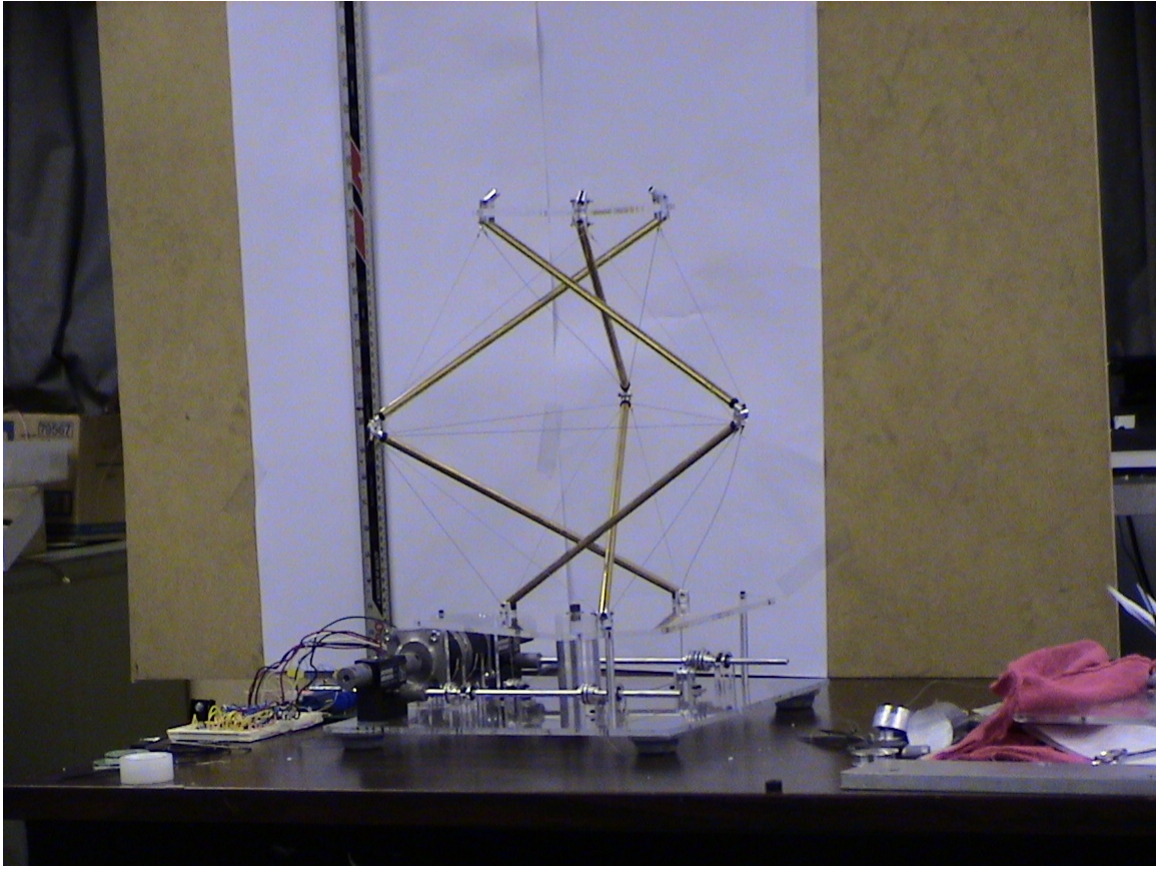
Figure 1.13 - Class 2 tensegrity mast

A Programmable Integrated Circuit (PIC) microcontroller and two stepper motors were used to actuate the deployment of the tower.
Each actuator controlled the lengths of three tendons for a total of six actuated tendons (Fig 1.14).
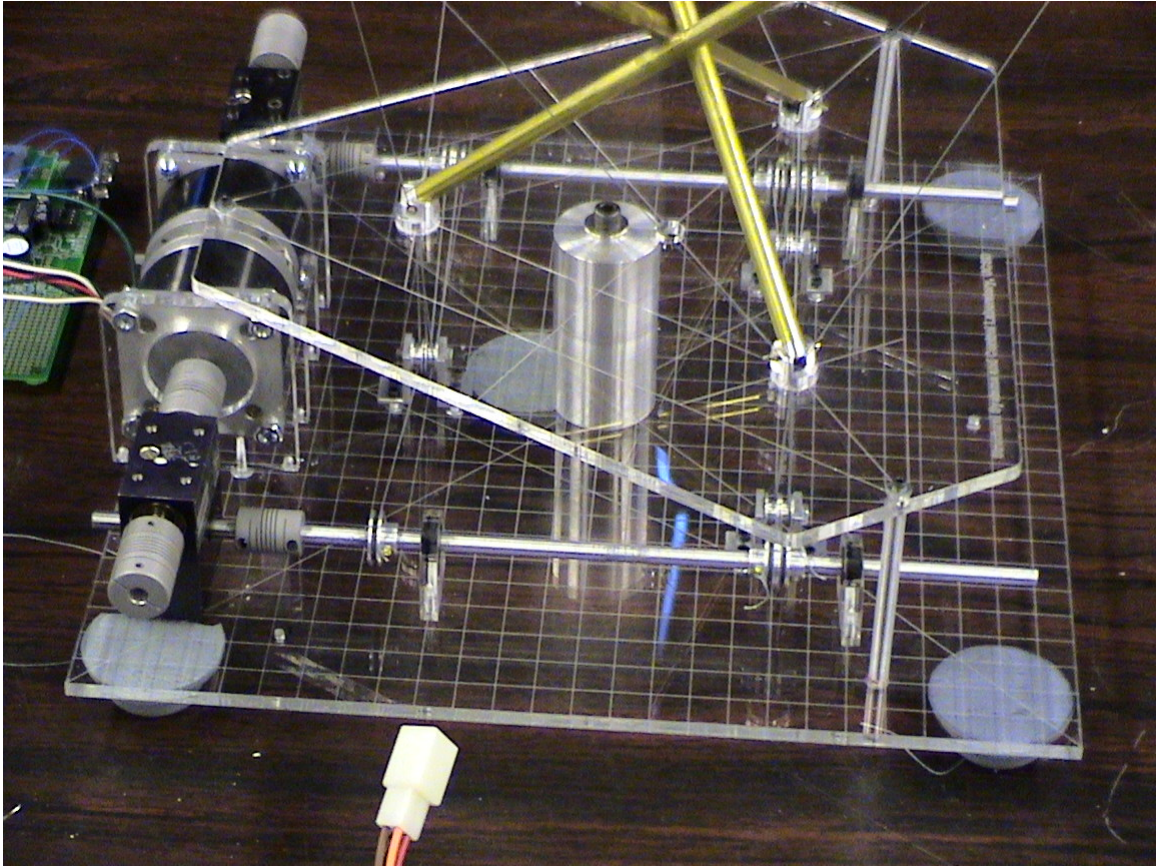
Figure 1.14 - Tendon actuating stepper motors.

By exploiting the modularity of the structure that enables a simplified equilibrium analysis, a solution for its equilibrium geometry was found. Based on this result, a string rest length open–loop control law was computed analytically. This control algorithm drives the structure through a sequence of configurations that remain in close proximity of the equilibrium manifold. Reconfiguration is accomplished in a quasi-static manner, ignoring dynamic effects.

Because of the limitations of the stepper motor and microcontroller, the motor commands (and therefore tendon length) are discrete and so cannot accurately implement a continuous trajectory (Fig 1.15). The blue graph and red dotted graph correspond to the lengths of the tendons controlled by the two actuators.
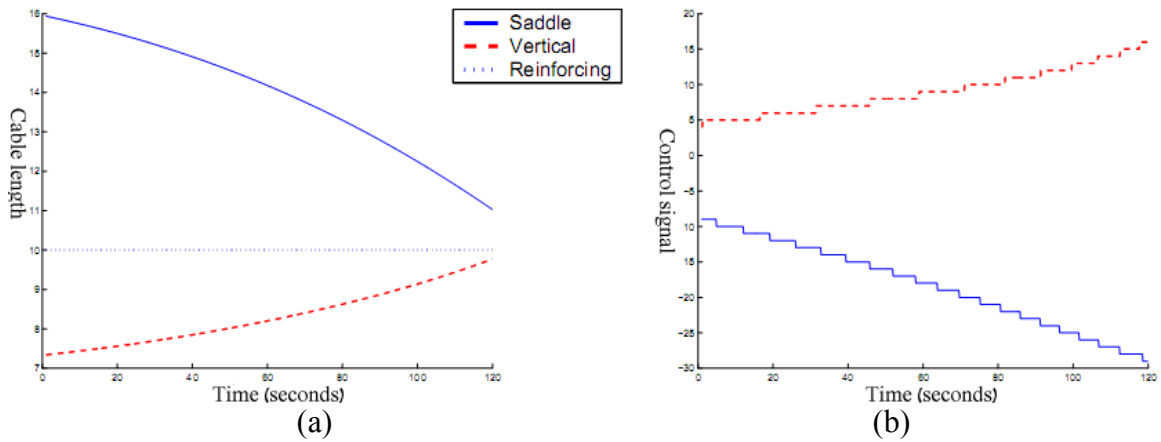
Figure 1.15 – Tendon trajectories for deployment (a) and stepper motor commands (b).

In contrast, the prototype device presented in this work uses six DC motors instead of the two stepper motors which allow it to implement a continuous trajectory and does not limit it to symmetric vertical deployment.

E. Fest et al. (2004) constructed the active structure shown in figure 1.16 at the Applied Computing and Mechanics Laboratory (IMAC) at the Swiss Federal Institute of Technology in Lausanne (EPFL).
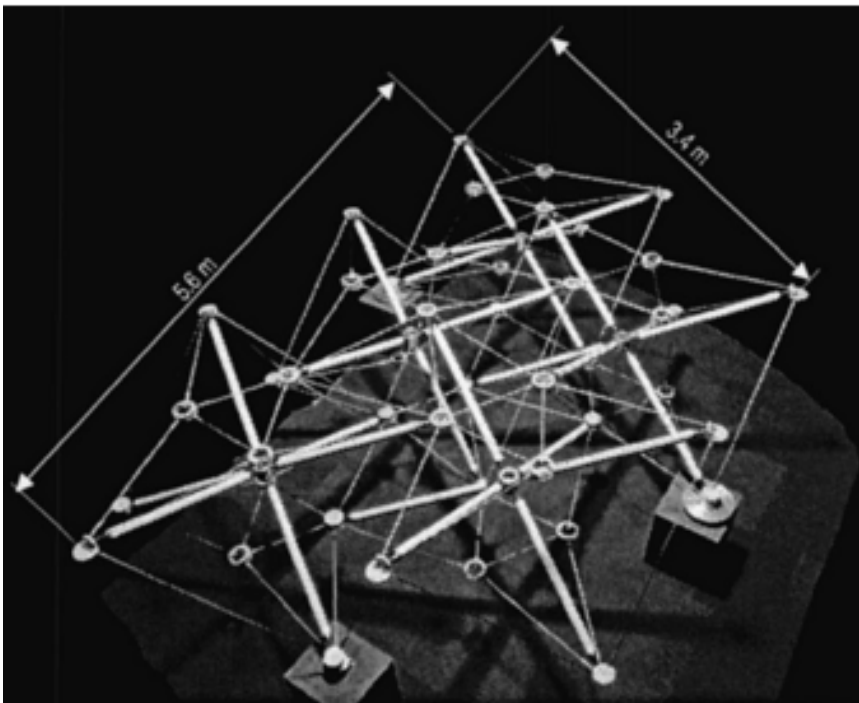

Figure 1.16 - Five module Tensegrity structure

The structure consisted of five modules arranged in an asymmetric configuration. Each module contained 6 struts and 24 cables. For the five module tensegrity, 30 telescopic

struts have the potential to be adjusted. The number of active struts has been chosen as 10.

Each actuator consistes of an electromechanical jack which produced linear energy from rotary energy. Rotary energy was created by an electric asynchronous motor via a bevel gear system (worm and wheel) and a screw nut system. Each actuator is equipped with a LVDT to measure displacement of the piston. The LVDT was used as a feed back control sensor. For unpredictable situations, the piston stroke displacement is bounded by a displacement limiter which, when touched, shut off the motor (Fig. 1.17).
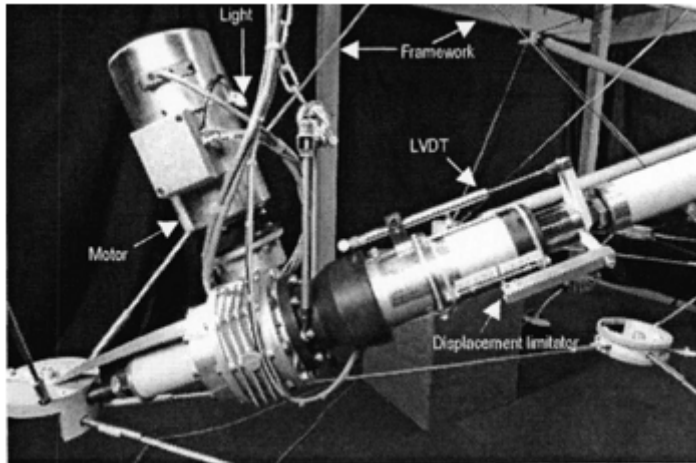

Figure 1.17 - Actuator and sensor

All the devices were multiplexed on a serial bus. The control area network (CAN) (Bosch 1993) bus, under CANopen protocol enabled one to communicate in real time between devices. Information is provided via a PC interface card run by a program written in LabView. The program permits automated application of a control command.

The goal of shape adjustment was to maintain the initial slope of the structure's upper level after a load has been applied to change it. The initial state of the structure was disturbed by a load. The structural response was then introduced as input to a search that included a predictive model.

The model was based on the geometry, topology and material properties of the structure analyzed using the dynamic relaxation method, a nonlinear analysis method, which has been shown to be reliable and accurate for this application by Fest et al. (2003).

The search is made by taking into consideration objectives and constraints, such as the slope and elastic limit of the cable. The search result consists of a set of strut elongations applied to the loaded structure. The new structural response was then measured to quantify the effectiveness of shape control.
Search time for most load cases was between one and ten minutes, while in extreme cases it could take less than 10 seconds or up to one hour.

Quasistatic control strategy, consisting of splitting the full command into increments and applying them strut by strut with simultaneous measurements, lead to a safe procedure for meeting the serviceability criterion and provided opportunities by which to identify potentially better commands leading to the full command.

C Paul et al. (2005a) at Cornell University introduced the concept of using a Tensegrity structure as the basis for land based locomotor robots. The Tensegrity robot shown in Fig. 1.18 demonstrated the ability to produce forward locomotion.

Figure 1.18 - Tensegrity locomotor robot

Aluminum tubes were used for the struts, and nylon covered rubber elastic cable was used for the cables. The transverse cables of the robot were actuated using servomotors mounted on the struts. During walking each servomotor was controlled to alternate between its maximum and minimum position value, producing an approximately 2cm change in the length of the cable.

The actuation strategy was developed using a simulated robot and a genetic algorithm. The control of the simulated robot was accomplished by periodically changing the rest lengths of the cables from the maximum to a minimum value. Each actuator was contracted once during each gait cycle. The point in the gait cycle at which the actuation began, the duration of the contraction, and its amplitude were determined by the genetic algorithm independently for each actuator. The period of the gait is also determined by a genetic algorithm. The genetic algorithm and simulation were also used to explore strategies involving different actuation amplitudes although in the physical robot only fixed 2 cm amplitudes were used. During evolution each individual is evaluated for 10,000 time steps in a dynamics simulation. The initial condition for each individual at the first time step is at position [0, 0] in the x-y plane. The fitness of the individual is

determined at the end of the evaluation period, and is considered to be the distance traveled in the y-direction with respect to the origin.

This Tensegrity based robot was not suitable for high precision movements. Due to the low pre-stress conditions which enable sufficient kinematic maneuverability the structure was subject to significant vibrations, which require high bandwidth control to subdue. Thus, only tasks which can tolerate a certain measure of imprecision in trajectory tracking, or which obviate the need for trajectories are suitable for it. Locomotion represents a suitable task domain as joint trajectories are not always particularly important, as long as the movement produces a non-zero motion of the center of mass in the appropriate direction (Fig 1.19).
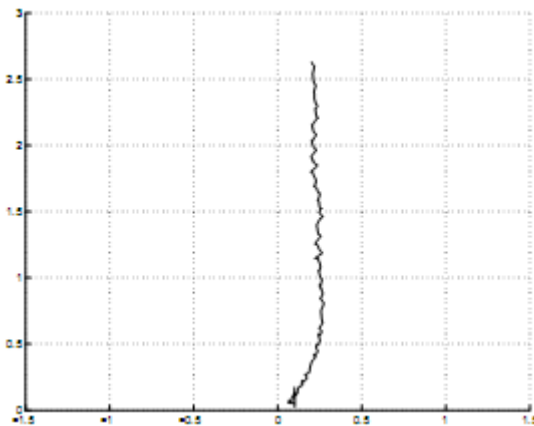

Figure 1.19 - The trajectory of the Center of Mass.

Further studies by Paul et al. (2005b, 2006) showed that multiple control strategies existed for forward locomotion, and that qualitatively similar behavior could be obtained with significantly different control strategies.

1.7 The present work

The objectives of the present work was to create a prototype device based on the tensegrity principle and to use it to experiment with a new method of actuation that allows operation comparable with conventional rigid robots in terms of flexibility and speed while maintaining the advantageous properties of tensegrity.

This research took advantage of the special properties associated with the device's topology to develop a new control strategy. Traditional control strategies require the synchronization of all of the device's member's lengths to maintain its stiffness. This new strategy uses control of only one member to assure the device's stiffness while the other members can be controlled independently and arbitrarily. This decoupling of the control of the members makes the control of the device very robust, as well as requiring little time and computing power.

Because a huge family of topologies, the Assur Graphs, shares the special properties of device's topology, the new control strategy is applicable to an infinite number of other devices.

1.8 Organization of the Thesis

In section 2 a discussion of the new shape change algorithm, the theoretical principle behind it and how it is used for controlling the device is presented. In section 3 one can find a presentation of the prototype device and its mechanical, electronic and software components. Section 4 is dedicated to the experiments preformed for this work and their results.

The conclusions reached in the course of this work and suggestions for further study are discussed in section 5.

2. Shape change algorithm theoretical background

The device studied in this research has a topology which belongs to a group of topologies that is called Assur Graphs. In this section Assur Graphs are introduced and some of their special properties are described. These special properties were used to develop and implement the shape change algorithm for the device.

2.1. Assur Graphs

In this section the concept of Assur Graphs is introduced. Assur Graphs' main properties are discussed as well as what distinguishes them from regular determinate trusses.

Figure 2.1 shows the topology of the device explored in this work. This topology is a three dimensional determinate truss but belongs to a special class of determinate trusses, termed Assur Graphs. All the structures that are Assur Graphs possess unique engineering properties, part of them have been used to develop the control system reported in the thesis.
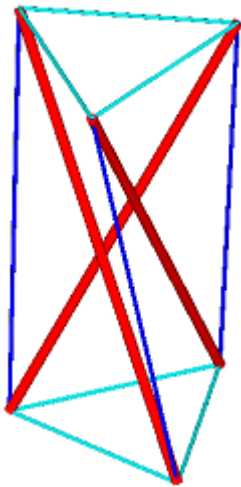

Figure 2.1 – The topology of the device – 3D Triad.

The concept of Assur Graphs was developed by Professor Leonid Assur at the Saint-Petersburg Polytechnic Institute. When first published in 1914, Assur's concepts (Assur 1952) did not receive much attention, but in 1930 I.I. Artobolevskii, a leading member of the Russian academy of sciences, adopted Assur's approach and employed it in his widely used book (Artobolevskii 1951). From that time on Assur Groups were widely employed in Russia and other eastern European countries.

The definition of Assur Graph:
Let G be a statically determinate graph. G is an Assur Graph IFF there is no sub-graph G' that is a statically determinate graph.

Figure 2.2 shows two 2D determinate graphs (a, b). Graph (b) has a sub graph of members, consisting of O1, A and O2, which is a determinate graph itself as shown in (c). This proves that graph (b) is not an Assur Graph. Graph (a) called Triad, doesn't have a sub graph of members which is a determinate graph and therefore it is an Assur graph.
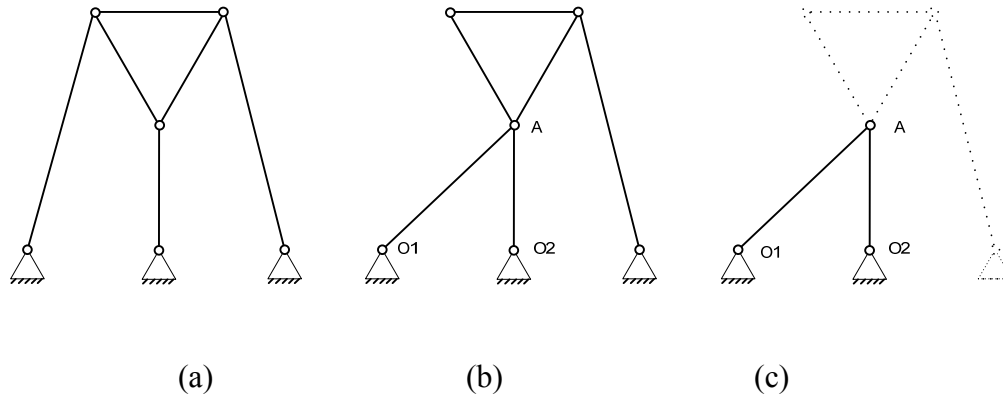

(a)   (b)   (c)

Figure 2.2 – Assur Graph - Triad (a), determinate graphs (b) and its sub graph (c).

Note: although for clarity this example (as well as others in this section) is given in the two dimensional space, the Assur Graph theory is valid for three dimensions as well. Figure 2.3 shows the 3D version of the Triad (a) as well as another 3D graph, the Tetrad (b). Neither of them has a determinate graph sub graph and therefore both are Assur graphs.

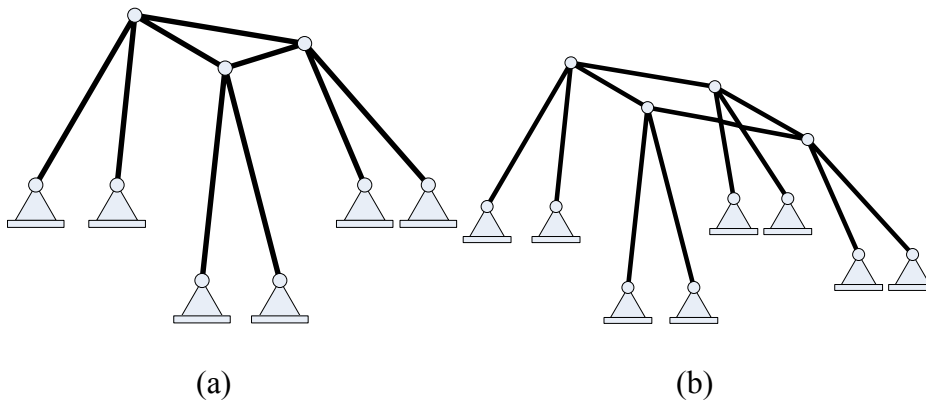(a)   (b)

Figure 2.3 – 3D Assur Graphs - Triad (a) and Tetrad (b).

Every determinate graph which is not an Assur Graph can be decomposed into sub-structures; each is an Assur Graph (Servatius et al., 2009). For example, the determinate trusses shown in figure 2.2b can be decomposed into three Dyad type Assur Graph (Figure 2.4).
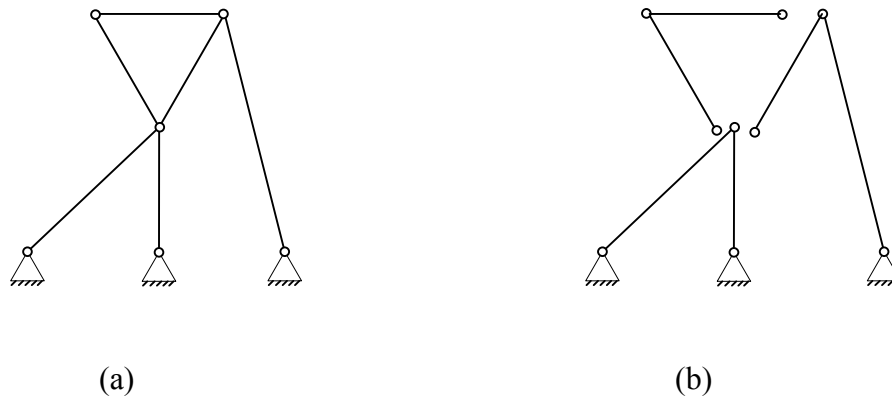
Figure 2.4 – Determinate graph (a) and its decomposition to Assur Graphs (b).

Assur Graphs have several special properties which make them ideally suited to form the topology of adjustable deployable tensegrity devices, the type reported in the thesis. The following properties exist in every Assur Graph, and during the research they were found to be useful in developing the shape control algorithm. The following theorems relate to the unique properties of the singularity in Assur Graphs.

Theorem 1(Servatius et al., 2009):

A pinned graph G has a realization p such that

1. G(p) has a unique (up to scalar) self-stress Λ which is non-zero on all edges; and

2. G(p) has a unique (up to scalar) first-order motion, and this is non-zero on all inner vertices;

IFF G is an Assur graph.

Figure 2.5 shows a Triad in a generic configuration (a) and a singular configuration (b) and its associated self stress (c) and joint mobility (d).
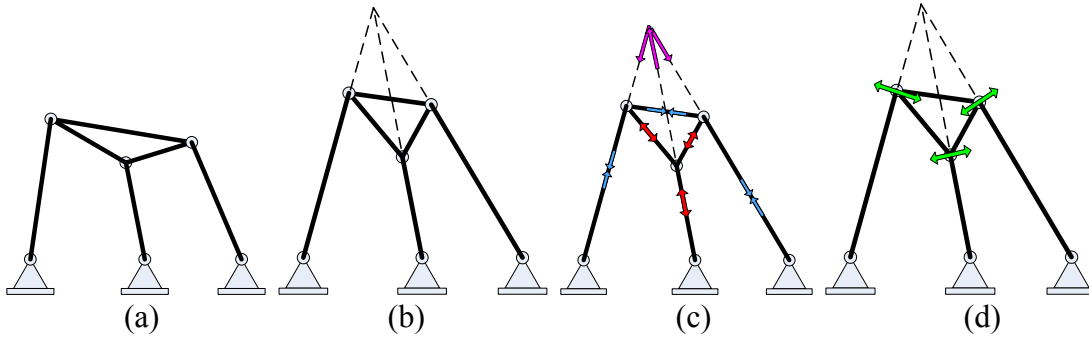
Figure 2.5 - Triad in a generic configuration (a), singular configuration (b), self stress forces (c) and joint mobility (d).

Figure 2.6 on the other hand, shows a determinate truss in three configurations. Configuration (a) is a generic configuration and has no self stress and no mobile joints. Configuration (b) has a unique self-stress in all the rods but only joint B is mobile (marked with vertical arrows). For configuration (c), joints A and B are mobile, but there is no unique self stress (for example it is possible to have a force F in edge 1, resisted by a Force –F in edge 2 and zero forces in edges 3 and 4).
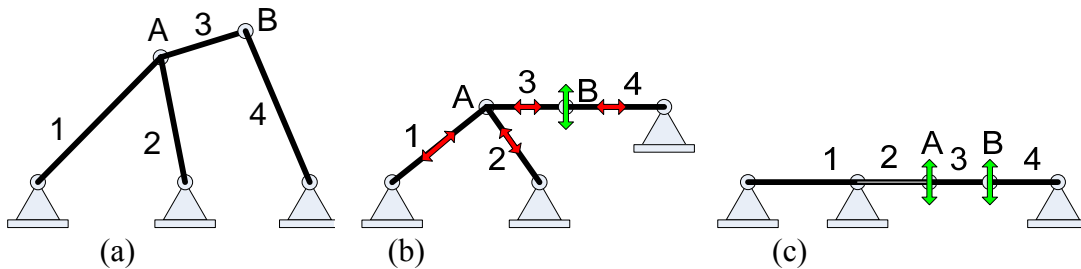

Figure 2.6 –Configurations of a determinate truss; a generic configuration (a), a uniquely self-stressed configuration (b), and a configuration with full joint mobility (c).

The meaning of this theorem is that each Assur Graph has a realization, such that the Assur Truss is at the singular configuration in which all the rods are stressed. If the rods in tension are replaced with cables then the structure becomes a rigid tensegrity. The significance of this theorem is that in a tensegrity device based on an Assur Graph, if one member is stressed then **ALL** of the members are stressed and the device is rigid.
In other words, to determine whether an Assur Truss in a singular configuration or not, it is sufficient to check only if one member is stressed.

Theorem 2 (Shai et al., 2010): Let T be an Assur Truss in a generic position. For every ground bar Bi there exists a length Li such that Assur Truss T', generated by replacing bar Bi with a bar Bi' with a length of Li, is in a singular configuration.

According to this theorem, it is possible to make any Assur Truss' configuration into a singular one simply by changing the length of any one of its ground bars. Figure 2.7 demonstrates this by using a Dyad type truss whose singular configuration is characterized by bars 1 and 2 being collinear. Dyad (a) which is in a generic configuration can be moved into a singular configuration in two ways; either by changing the length of bar 1 (b) or by changing the length of bar 2 (c).
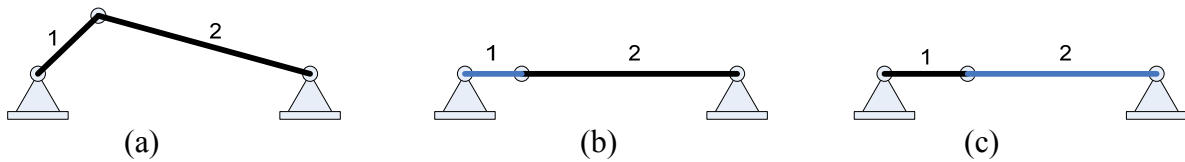

Figure 2.7 - Dyad in generic configuration (a) and singular configurations (b,c).

Another example is presented in Figure 2.8 which shows a common Assur Truss, a Triad. The Triads's singular configuration is characterized by lines a, b, c that are the continuation of lines 1,2,3, respectively, intersecting at the same point. By changing the length only of edge 1, the Triad is moved from a generic configuration (Figure 2.8a) to a singular configuration (Figure 2.8b) in which a, b and c intersect at a single point.
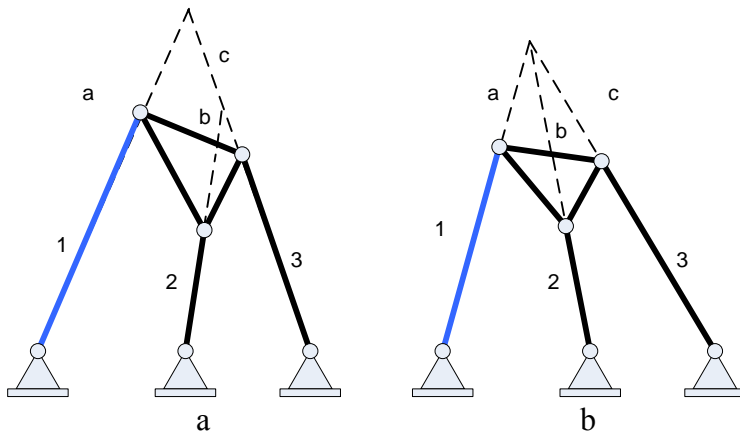

Figure 2.8 - Triad in generic configuration (a) and the singular configuration (b) resulting from changing the length of edge 1.

A third example is presented in Figure 2.9 which shows a more complex Assur Truss, a Tetrad. The Tetrad's singular configuration is characterized by points a (the intersection of lines 2 and 3), b (the intersection of lines 1 and 4) and c (the intersection of lines 5 and 7) being collinear. By changing the length only of edge 1, the Tetrad is moved from a generic configuration (Figure 2.9a) in which points a, b and c are no collinear to a singular configuration (Figure 2.9b) in which a, b and c are collinear.

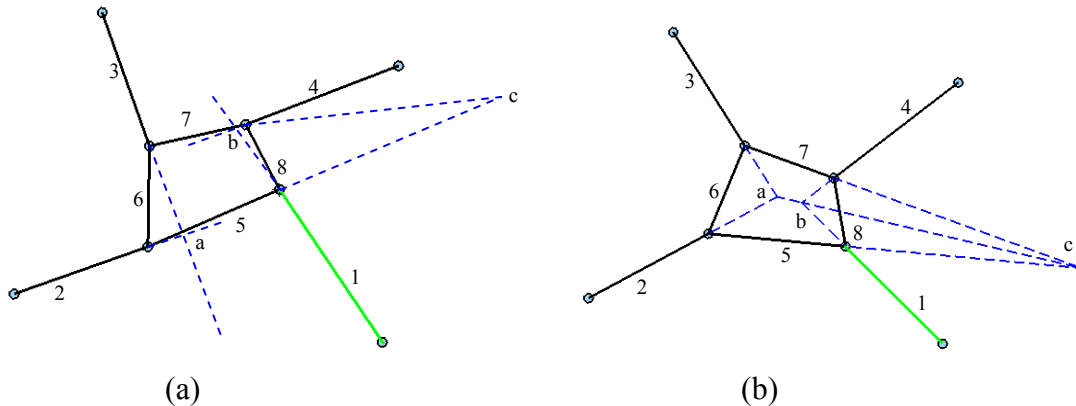(a)   (b)

Figure 2.9 - Tetrad in a generic configuration (a) and the singular configuration (b) resulting from changing the length of edge 1.

When an Assur Truss A is in its singular position, a force F may be assigned to one of its members, the forces on all other members will be proportional to F. Members with positive force (tension) may be replaced with cables and members with negative force (compression) with struts to create a tensegrity device T. If a force of –F is assigned to the same member, then in the resulting tensegrity device T', each member that is a cable in T will be a strut and each member that is a strut in T will be a cable. An example of A, T and T' for the Dyad Assur Graph are presented in figure 2.10.

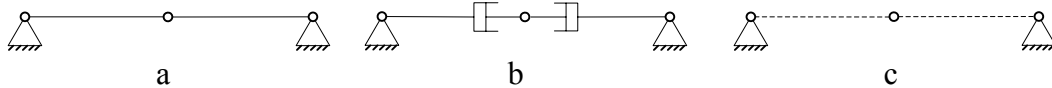a   b   c

Figure 2.10 - Dyad Assur Graph A (a) and its two possible tensegrity devices T (b) and T' (c).

Because both T and T' are in the singular configuration both are in equilibrium which provides them with stiffness. However, one of them is in a stable equilibrium, which means that if the equilibrium is disturbed the device will return to its equilibrium state, while the other is in an unstable equilibrium which will drift away from the equilibrium state if disturbed. Figure 2.11 shows two Dyad tensegrity devices' reaction to disturbance. The light arrows represent the member forces acting on the joint and the dark arrows represent the movements of the joint first because of the disturbance and then because of the acceleration caused by the forces exerted by the members. The device on the left is composed of two struts and its equilibrium is unstable, while the device on the right is composed of two cables and its equilibrium is stable.
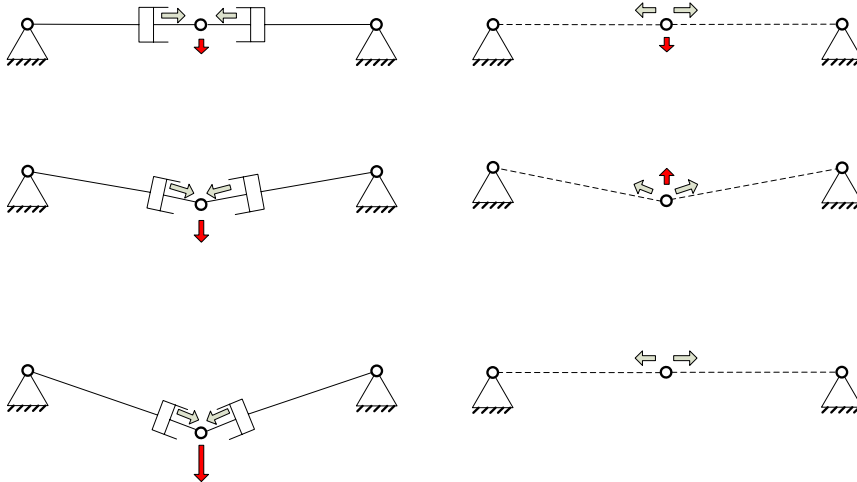
Figure 2.11 – Unstable (left) and stable (right) Dyad tensegrity devices' reaction to disturbance.

For the purpose of this research the following method was used to determine which of the two possible tensegrity devices will yield a stable equilibrium:

- Arbitrarily select a generic configuration for the device.
- Arbitrarily select one of the device's ground links.
- Change the length of the selected ground link until the device reaches its singular configuration.
- If the link's final length is shorter than its starting length then assign to it a positive force F (tension) and if the link's final length is longer than its starting length then assign to it a negative force F (compression).
- Calculate the forces in all the other members.
- For a tensegrity device in a stable equilibrium, every member with a positive force should be a cable and every member with a negative force a strut.

Figure 2.12 demonstrates the process of creating a tensegrity device in stable equilibrium from the Triad shown in figure 2.9. Figure 2.12 (a) shows a generic configuration of the triad with ground link 1 selected. The Triad is moved to a singular configuration by shortening ground link 1 (b). Since ground link 1 was shortened, it is assigned a positive (tension) (c). Figure 2.12 (d) shows, the forces in the other links, either positive forces (tension) represented by light arrows or negative forces (compression) represented by dark arrows. Finally (e) shows the resulting stable device when the links in tension are replaced by cables and the links in compression are replaced by struts.
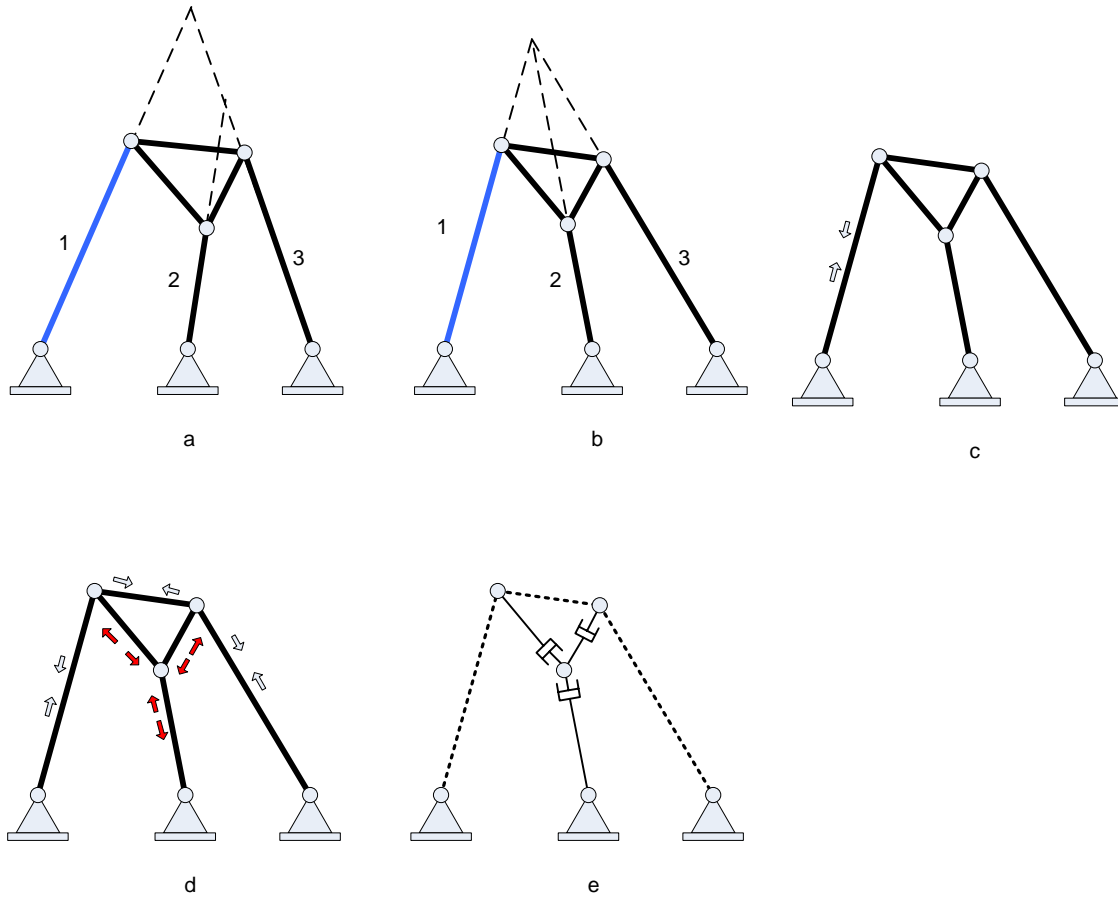
Figure 2.12 – Determining a Triad's stable form by using a generic configuration (a), achieving a singular configuration by shortening a ground link (b), assigning a positive force to the link (c), deriving the forces on the other links (d) and finally replacing the links with struts an cables to get a device in stable equilibrium (e).

Another important property of Assur Graphs which is very important to this research is that there is an infinite number of them and therefore the results are applicable to an infinite number of devices. Assur Graphs can be ordered in a table with infinite numbers of rows and columns; this order is termed the *canonical form* (Shai, 2009) of Assur Graphs. The canonical form of two Assur Graphs is proved to be an ordered hierarchy of several levels, enabling systematic generation of all its members.
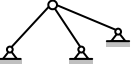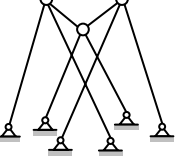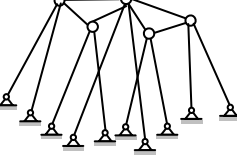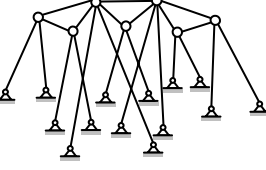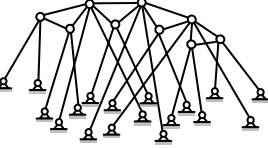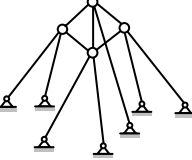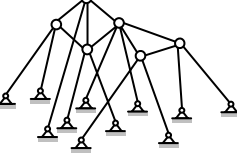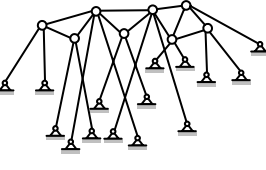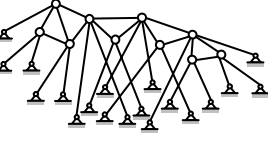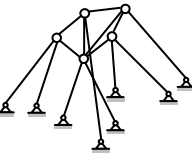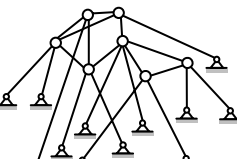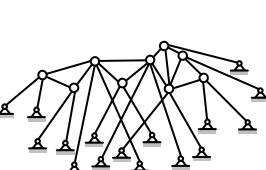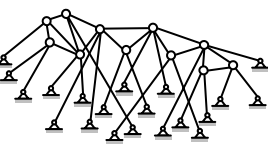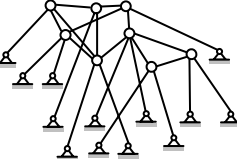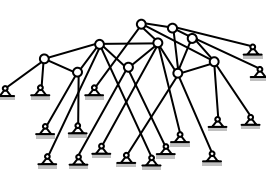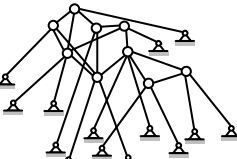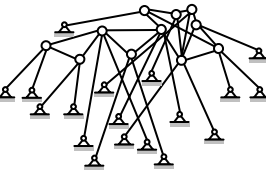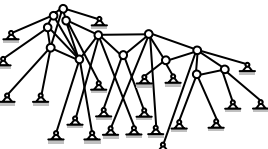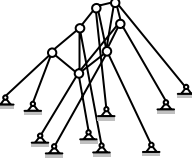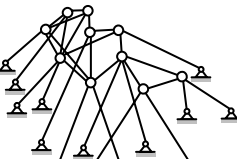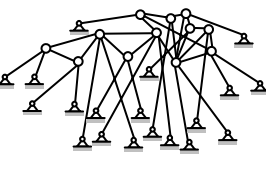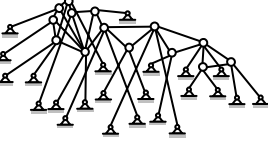
Using the canonical forms table or the methods developed to produce it, finding topologies for tensegrity devices as can be accomplished quickly and efficiently.

The simplest (in terms of number of members) Assur Graphs are presented in table 2.1 (2D) and 2.2 (3D) which can be considered as the beginning of the complete canonical forms tables.

Table 2.1- Assur Graphs in 2D

Table 2.2 – Assur graphs in 3D

Class 1	Class 2	Class 3	Class 4	Class 5

Assur Graph's above mentioned properties form the basis of prototype device control algorithm. First of all, the device topology was selected from the three dimensional canonical form to make sure it is an Assur Truss thus has the special properties. Following theorem 2, one member's length is adjusted to bring the devices geometry into a singular configuration and at all time one member's stress is monitored to make sure the device stays in a self stressed singular configuration.

2.2 Shape change algorithm

The objective of the shape change algorithm is to allow the device to move from one singular position to another while maintaining its stiffness at all times. The shape change is accomplished by changing the length of the device's actuated members (cables and/or struts). For the device to maintain its stiffness throughout its shape change, all of its members must be stressed. According to theorem 1, forces in all of its members exist IFF the device is in a self stress position. The latter state is achieved by making sure that the device is in a singular position all the time.

It will be proved that when all but one of the device's members are at any arbitrary lengths, the device can be placed in a singular position by setting the length of the remaining member to a specific length. That member will be referred to as the *force controlled member*, and all the other actuated members as the *position controlled members*.

Based on that fact, an algorithm was developed in which the position controlled members change their length from the starting length to their length in the new shape in some arbitrary fashion, while the force controlled member is actuated in a way that will maintain the device's stiffness.

Theorem 3
If a triad tensegrity device is in a singular position then the length of one member is dictated by the lengths of the other members.

Proof:

Without loss of generality the proof will show that the length of member 1 is a function of the lengths of the other members. It is easy to verify that the same proof can be used if any other member of the triad was selected. For clarity this theorem will first be proved in 2D and then will be proved in 3D.

Symbols used in the proof:
Constants (the ground points coordinates and members' lengths):

O_{ik} Ground point O_i's k coordinate (x or y in 2D)

|JK| The length of the element between joints J and K other than $|O_1A|$

Variables:

J_k Point J's k coordinate. The points are A,B,C and S.

2D case

The topology of a 2D triad, which is the 2D equivalent of the 3D T-3 tensegrity prism, is shown in fig. 2.13, where the vertices A,B,C and the edges 1-6 correspond to the joints and the elements, respectively.
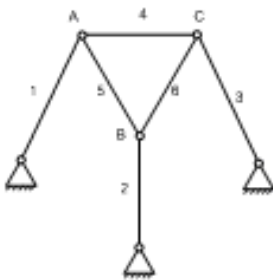
Fig. 2.13 2D triad topology.

This topology can be used to construct a 2D Tensegrity device by replacing edges 1, 3 and 4 with cables and edges 2, 5 and 6 with struts, as shown in Figure 2.14.
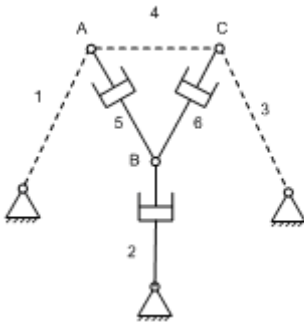
Fig. 2.14 Triad Tensegrity device.

The tensegrity device's stiffness is maintained because it is in a singular configuration which allows self stress.

The triad singular position is characterized as follows:
Triad is in a singular position IFF the continuations of the ground elements, those elements connected to the ground, intersect at the same point.

For the triad tensegrity device appearing in Figure 2.14 it means that the continuation of elements 1, 2 and 3 should all intersect at the point s as shown in Figure 2.15.
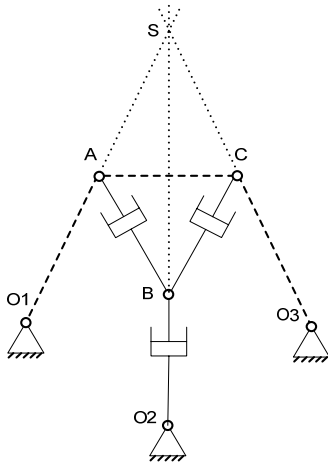
Fig. 2.15 Singular configuration of a triad Tensegrity device.

Line *(O₁ A S)* contains points O_1, A and S which means that their projective geometry coordinates are linearly dependant and that the determinant of the matrix containing them equals zero.
The same is true for lines *(O₂ B S)* and *(O₃ C S)* and is described by (2.1).

$$(2.1)$$

$$\begin{vmatrix} O_{1x} & A_x & S_x \\ O_{1y} & A_y & S_y \\ 1 & 1 & 1 \end{vmatrix} = 0$$

$$\begin{vmatrix} O_{2x} & B_x & S_x \\ O_{2y} & B_y & S_y \\ 1 & 1 & 1 \end{vmatrix} = 0$$

$$\begin{vmatrix} O_{3x} & C_x & S_x \\ O_{3y} & C_y & S_y \\ 1 & 1 & 1 \end{vmatrix} = 0$$

The following 5 geometric equations describe the lengths of elements 2 to 6:

(2.2)

$$|2|=|O_2B|=\sqrt{(O_{2x}-B_x)^2+(O_{2y}-B_y)^2}$$

$$|3|=|O_3C|=\sqrt{(O_{3x}-C_x)^2+(O_{3y}-C_y)^2}$$

$$|4|=|AB|=\sqrt{(A_x-B_x)^2+(A_y-B_y)^2}$$

$$|5|=|AC|=\sqrt{(A_x-C_x)^2+(A_y-C_y)^2}$$

$$|6|=|CB|=\sqrt{(C_x-B_x)^2+(C_y-B_y)^2}$$

By solving these 8 equations it is possible to calculate all eight variables (A_x, A_y, B_x, B_y, C_x, C_y, S_x and S_y). Once we have the value of the variables we can calculate the length of the force controlled element, in this case cable 1 (2.3). This can be done since the coordinates of O_1 were constants and those of A were found by solving the above equations.

(2.3)

$$|1|=|O_1A|=\sqrt{(O_{1x}-A_x)^2+(O_{1y}-A_y)^2}$$

Therefore it is shown that member 1's length is a function of the lengths of the other members, as long as the device is in a singular position.

3D case

The same method is used to prove the theorem for the 3D Triad. The topology of a 3D Triad, which is the T-3 tensegrity prism, is shown in figure 2.16:
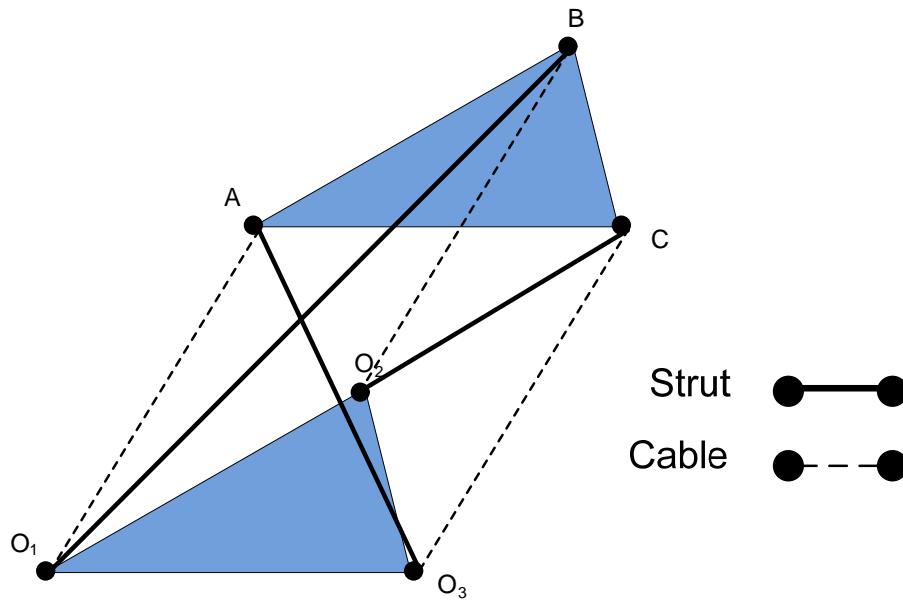
Figure 2.16 - A tensegrity structure based on the 3D triad.

The tensegrity structure's rigidity is maintained because it is in a singular configuration which allows the existence of a self stress.

The singular configuration for a 3D triad is characterized as a geometry in which 3 planes $\prod 1 = (O_1AO_3)$, $\prod 2 = (O_1BO_2)$ and $\prod 3 = (O_2CO_3)$, each defined by a strut and a cable (figure 2.17), intersect the plane defined by the top plate (ABC) at a single point S (figure 2.18).
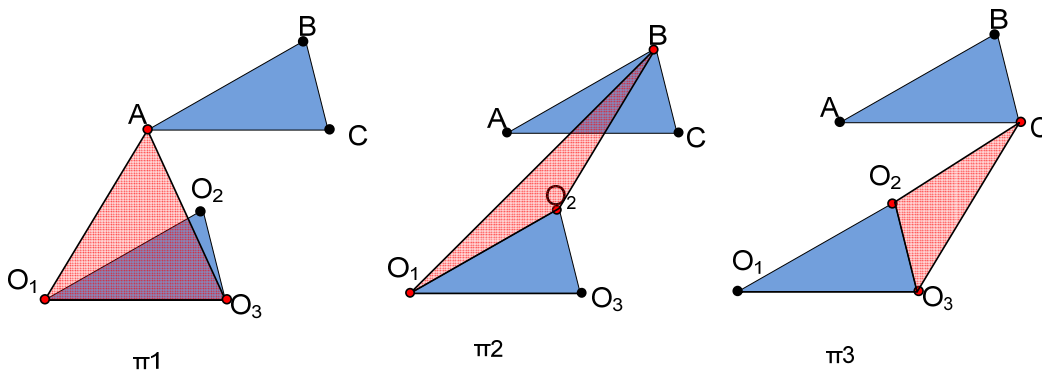
Figure 2.17 – The three planes $\prod 1$, $\prod 2$ and $\prod 3$.
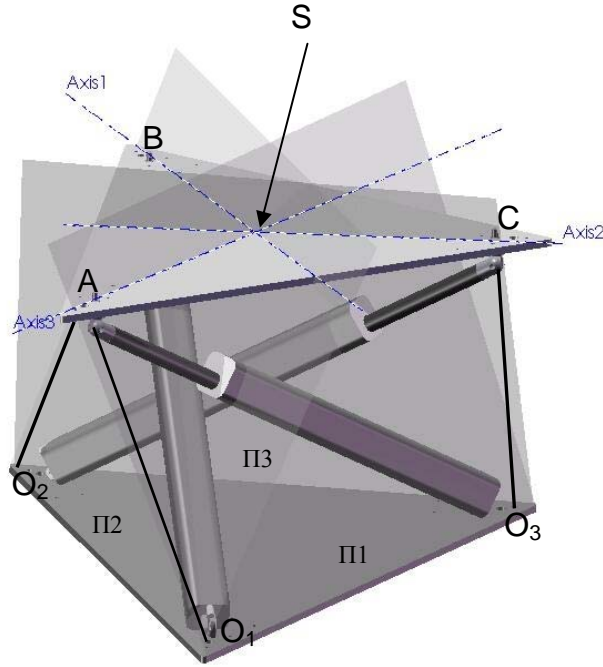
Fig. 2.18 A singular configuration of a T-3 tensegrity prism based device.

The proof will show that the length of member O_1A is a function of the lengths of the other members, but it is easy to see that the same proof can be used for any other member.

The following 4 projective geometry equations describe the planes (ABCS) , (O_1AO_3S), (O_1BO_2S) and (O_2CO_3S):

$$(2.4)$$

$$A \vee B \vee C \vee S = \begin{vmatrix} A_x & B_x & C_x & S_x \\ A_y & B_y & C_y & S_y \\ A_z & B_z & C_z & S_z \\ 1 & 1 & 1 & 1 \end{vmatrix} = 0$$

$$O_1 \vee A \vee O_3 \vee S = \begin{vmatrix} O_{1x} & A_x & O_{3x} & S_x \\ O_{1y} & A_y & O_{3y} & S_y \\ O_{1z} & A_z & O_{3z} & S_z \\ 1 & 1 & 1 & 1 \end{vmatrix} = 0$$

$$O_1 \vee B \vee O_2 \vee S = \begin{vmatrix} O_{1x} & B_x & O_{2x} & S_x \\ O_{1y} & B_y & O_{2y} & S_y \\ O_{1z} & B_z & O_{2z} & S_z \\ 1 & 1 & 1 & 1 \end{vmatrix} = 0$$

$$O_2 \vee C \vee O_3 \vee S = \begin{vmatrix} O_{2x} & C_x & O_{3x} & S_x \\ O_{2y} & C_y & O_{3y} & S_y \\ O_{2z} & C_z & O_{3z} & S_z \\ 1 & 1 & 1 & 1 \end{vmatrix} = 0$$

The following 8 geometric equations describe the lengths of lines 2 to 6:

(2.5)

$$|AB| = \sqrt{(A_x - B_x)^2 + (A_y - B_y)^2 + (A_z - B_z)^2}$$

$$|BC| = \sqrt{(B_x - C_x)^2 + (B_y - C_y)^2 + (B_z - C_z)^2}$$

$$|AC| = \sqrt{(A_x - C_x)^2 + (A_y - C_y)^2 + (A_z - C_z)^2}$$

$$|O_2 A| = \sqrt{(O_{2x} - A_x)^2 + (O_{2y} - A_y)^2 + (O_{2z} - A_z)^2}$$

$$|O_1 B| = \sqrt{(O_{1x} - B_x)^2 + (O_{1y} - B_y)^2 + (O_{1z} - B_z)^2}$$

$$|O_2 B| = \sqrt{(O_{2x} - B_x)^2 + (O_{2y} - B_y)^2 + (O_{2z} - B_z)^2}$$

$$|O_2 C| = \sqrt{(O_{2x} - C_x)^2 + (O_{2y} - C_y)^2 + (O_{2z} - C_z)^2}$$

$$|O_3 C| = \sqrt{(O_{3x} - C_x)^2 + (O_{3y} - C_y)^2 + (O_{3z} - C_z)^2}$$

By solving these 12 equations it is possible to calculate the 12 variables.
Using the coordinates of O_1x, O_1y, O_1z, Ax, Ay and Az it is possible to calculate the length of member O_1A.

Therefore it is shown that member 1's length is a function of the lengths of the other members, as long as the device is in a singular position, as stated in theorem 3.

2.3 Implementation

When all of the device's members (referred to as the position controlled members) except one ground link (referred to as the force controlled member) are at any arbitrary lengths, the device can be placed in a singular position by setting the length of the one ground link to a specific length. It has been proved above for the device's Triad topology, but it is true for any tensegrity device whose topology is an Assur Graph.

45

Based on that, the following algorithm has been developed in which the position controlled members change their length from the starting length to their length in the new shape in some arbitrary fashion, while the force controlled ground link is actuated in a way that will make sure that its length is the required length for the device to be in a singular position.

The algorithm's inputs are the lengths of the position controlled members and the force in the force controlled member; its outputs are the command signals to the actuators.

The algorithm models the force controlled member as an elastic body and monitors the force in it to make sure it is in a length that is required for the singular configuration.

Suppose that the device is in a singular position such that the force controlled member's length is L_0 and it has a force of F_0 in it.
If the member's spring constant is K and its rest length is R_0, equation 2.6 must be satisfied.

(2.6)

$L_0 = R_0 + F_0/K$

Then there is a small change in the structure's shape such that the force controlled member must be at length L_1 for the device to be in a singular position. If the rest length stays at R_0 then the force controlled member will have a slightly different force F_1.

(2.7)

$L_1 = R_0 + F_1/K$

If the shape continues to change and the rest length remains at R_0 the force may either drop to zero (and self stress will be lost and the device will lose its stiffness) or the force may rise too much and the member or its actuator will fail. However, if the rest length will be changed to R1 so that (2.6) is satisfied, the force will return to F_0 and self stress will be maintained.

(2.8)

$L_1 = R_1 + F_0/K$

Therefore as long as force is maintained at F_0 (or close to it), the force controlled member will be at the required length to keep the device in a singular position.

That means that we can make sure that the force controlled member is at the required length by monitoring its force rather than its length. In fact it is not even necessary to know what the required length is to assure the device's stiffness.

Since we can change the force controlled member's rest length throughout the structure's movement so that the force in it is maintained, the device will have a singular shape at any given time and will maintain its stiffness throughout its movement.

Based on this principle the following algorithm was developed:

1. Starting condition for the algorithm is that the device is in a singular configuration.

2. Select a target shape for the device and extract from it the target member lengths. The target shape must be a singular configuration.

3. Select the desired force in the force controlled member. Because when the device is in a singular configuration a single self stress exists in it, the forces in all of the other members will be proportional to the force in the force controlled member.

4. Measure the current member lengths and calculate the length change required by each member to reach its target length by subtracting the current length from the desired length.

5. Based on the required length changes and the device's actuators speed, set a target time for reaching the target shape.

6. Generate a trajectory for each actuated member that starts with the current length and ends with required length at the target time. For the prototype device the generated trajectory was a sigmoid shaped curve that allowed the actuators to slowly accelerate from a rest to the desired speed and then gently decelerate until reaching a complete stop when the target time is reached.

7. Select one of the actuated members to be the force controlled member. In the prototype cable number 1 was arbitrarily selected as the force controlled member.

8. Activate the device's controllers in the following manner:

   The force controlled member's controller causes the force controlled member to maintain the desired force in it, thus assuring the device's stiffness.

   The position controlled members' controllers cause the members lengths to follow their defined trajectories, thus changing the device's shape into the desired one.

9. Once the target time has been reached, the position controlled members should be at their target lengths and according to the theorem, so should the force controlled member. The device can now be either deactivated or moved into a new singular configuration.

The advantage of this algorithm over most others is that it requires very little computation time. Only one singular configuration needs to be found (the target configuration), while most other algorithms require that many singular configurations be found, changing progressively from the starting configuration to the target configuration.

3. Experimental system

A tensegrity device has been developed to study the feasibility of a tensegrity based robot (fig. 3.1). The purpose of the device is to change its shape with five degrees of freedom while maintaining stiffness at all times. The device has been used to test various hardware components, shape change algorithm and control strategies.
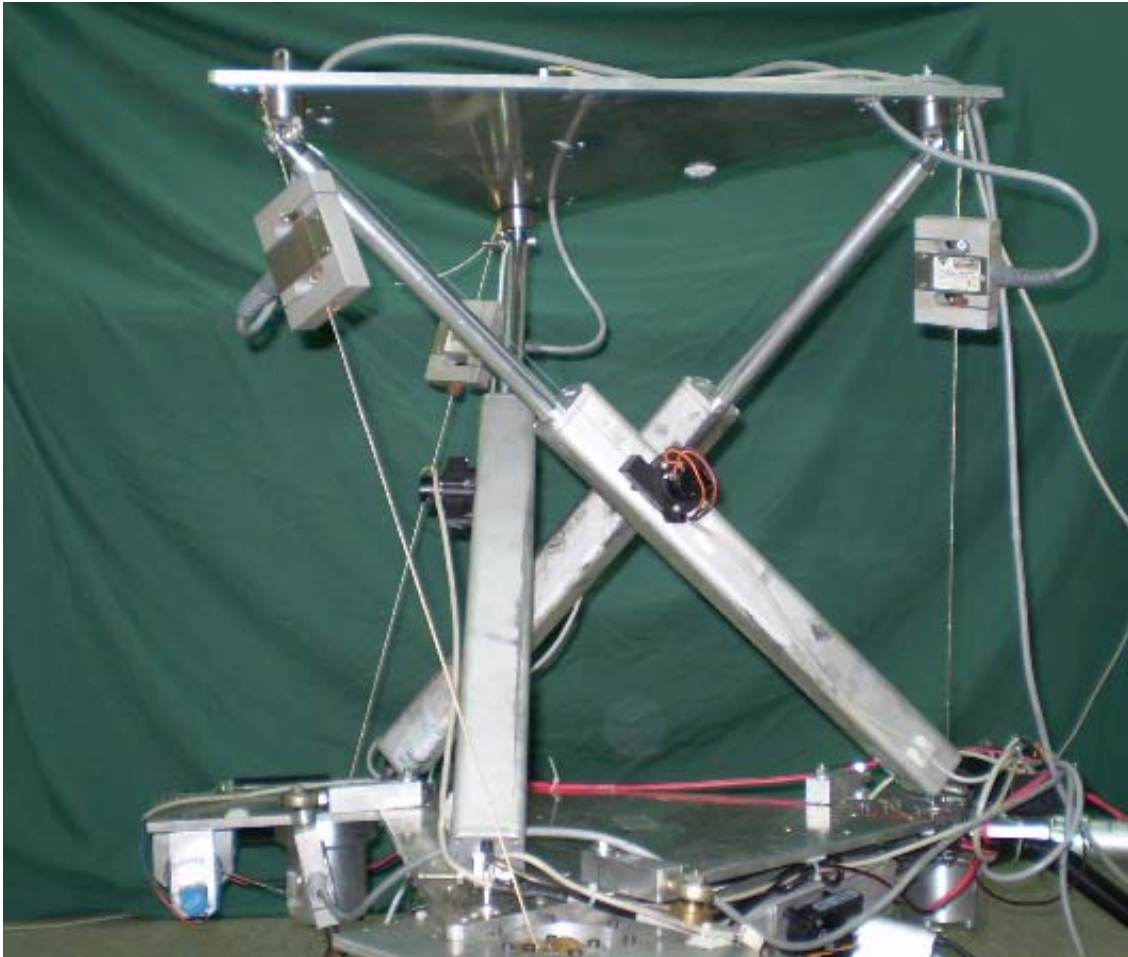
Figure 3.1: Prototype device photo.

3.1. Layout

The device's topology is one of the most basic Assur Graphs, the 3D Triad (Fig 3.2). In this variation of the 3D triad each joint to the ground is overlapped by another joint, this topology is known as a T-3 tensegrity prism. It is constructed of a top triangle whose edges are under tension connected by three struts and three cables to the ground.
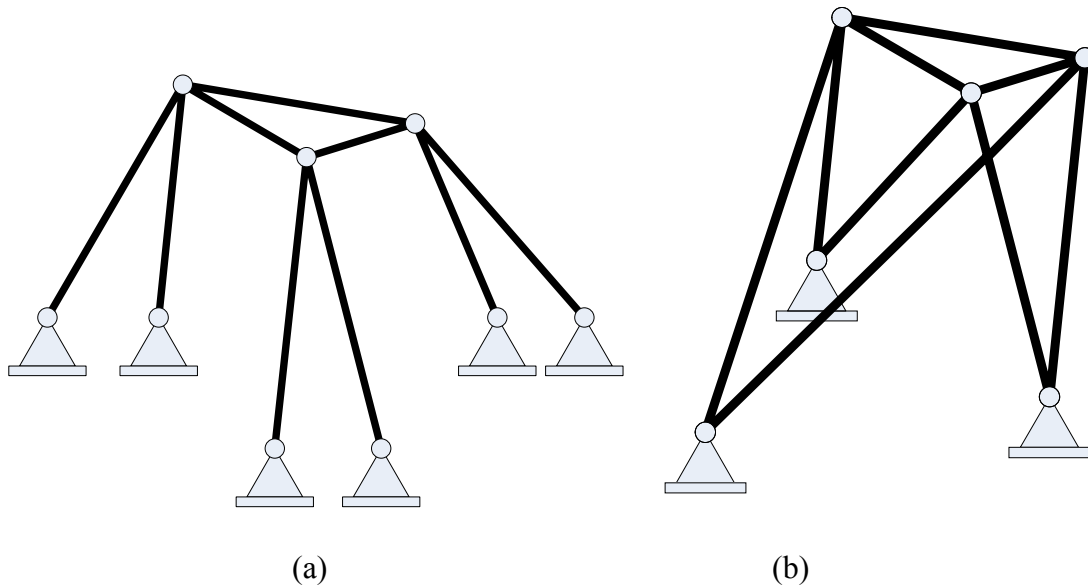
Figure 3.2: 3D Triad (a) generic form (b) T-3 tensegrity prism.

In the prototype device the top triangle and the ground are equilateral triangles measuring 460 mm per side. Each is made of an aluminum plate (instead of 3 cables) to allow mounting of sensors and actuators and carrying loads. The plates actually measure 560mm per side but the strut connection points are spaced 460mm apart from each other. Also, because of technical limitations, the points where the cables are attached to the top and bottom plates are close to the points where the struts are attached, but they do not coincide. Therefore, the prototype device's topology is not identical to the T-3 prism's, rather a close approximation of it.

The struts are electrically actuated cylinders with a compressed length of 472.5 mm and maximal extended length of 722.5 mm (Fig 3.3). The ends of each cylinder can twist in relation to one another. The cylinders are attached to the plates with double hinged joints similar to universal joints. The combination of a universal joint and the twist is equivalent to a spherical joint and gives the degree of freedom that the T-3 prism has (except for the trivial motion of each strut, the rotation around its own axis). The double hinged joints are in fact a quadruple hinged joint design that can be used to connect 2 struts to the plate at the same point, one to its upper side and another to its bottom side each with its own two independent degrees of freedom (fig 3.4). The purpose of this design is to allow several devices to be connected together to form a multi staged tensegrity mast (fig 3.5).

Figure 3.3: Cylinders - compressed (top) and extended (bottom).

| a | b | c |
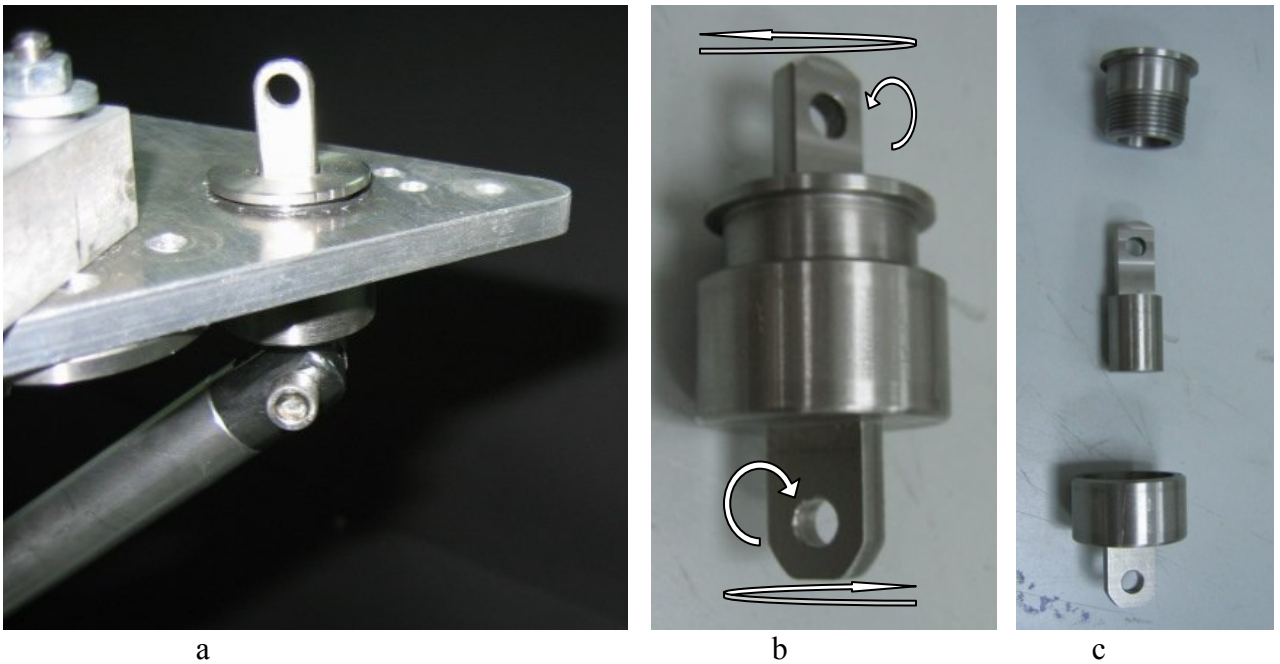
Figure 3.4: Quadruple hinged joint joint (a) mounted with one strut attached (b) showing degrees of freedom (c) disassembled.

Figure 3.5: Three-staged Class 2 mast prototype.

The cables are 1.5 mm in diameter steel braided cables, at one end fixed to a plate and at the other to a winch-like electric actuator which is connected to the other plate. The actuator can release and reel in the cable to vary it effective length.

3.2. Control hardware

Various electro mechanical components are used to change the shape of the mast (fig.3.6)
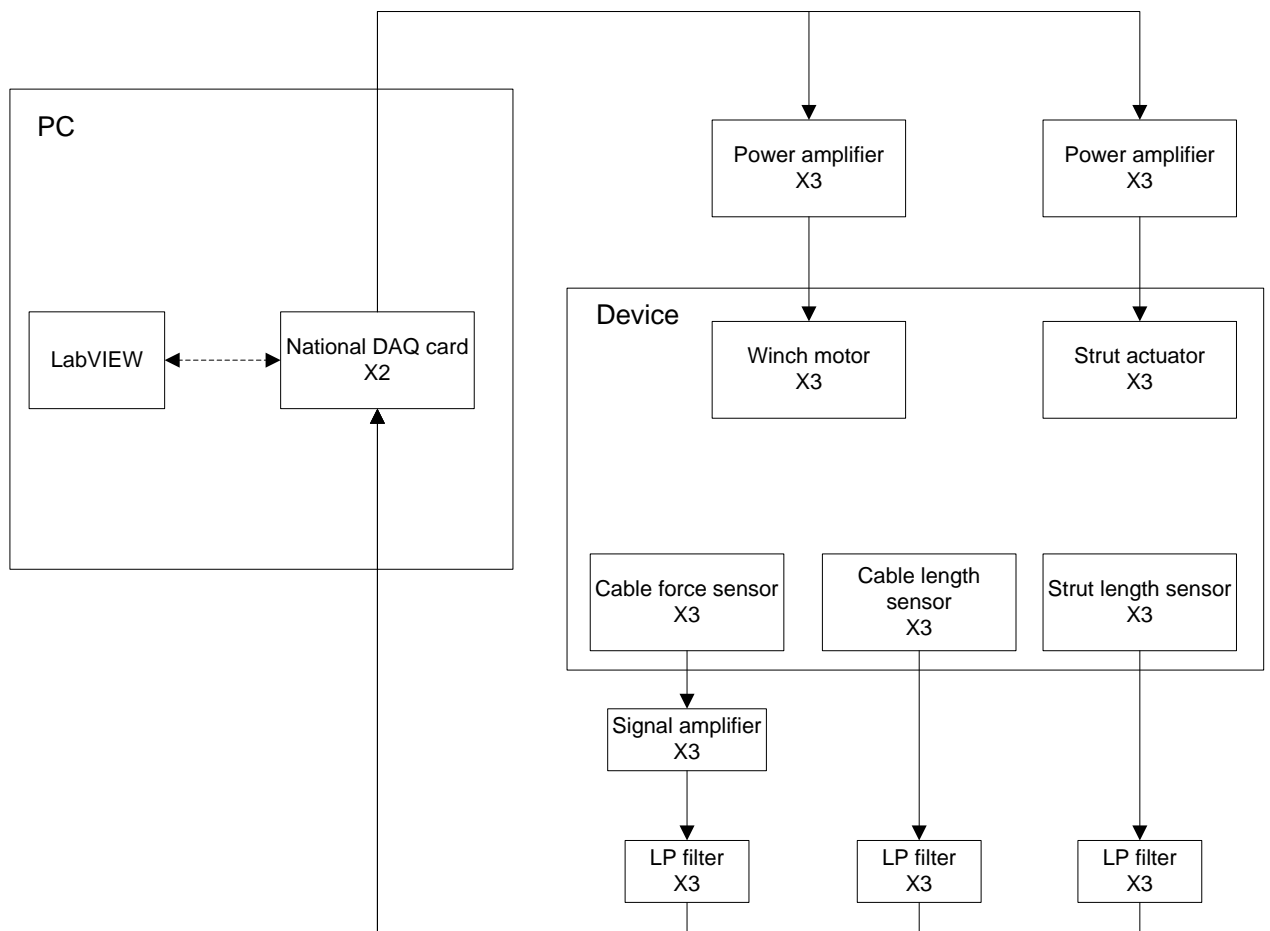
Figure 3.6: Device components block diagram.

There are 2 types of actuators in the device, the struts which are commercially available electrical linear actuator and the bespoke winches that control the cables' lengths and

tensions (figure3.7). In the winch, the cable (A) around a drum (B) which is powered by a DC motor (C). It is routed through a system of three guidance pulleys (D) inside an aluminium case (E). The guidance pulleys are used to make sure that the cable always exits the winch from the same point, regardless of how much of it is coiled around the drum.
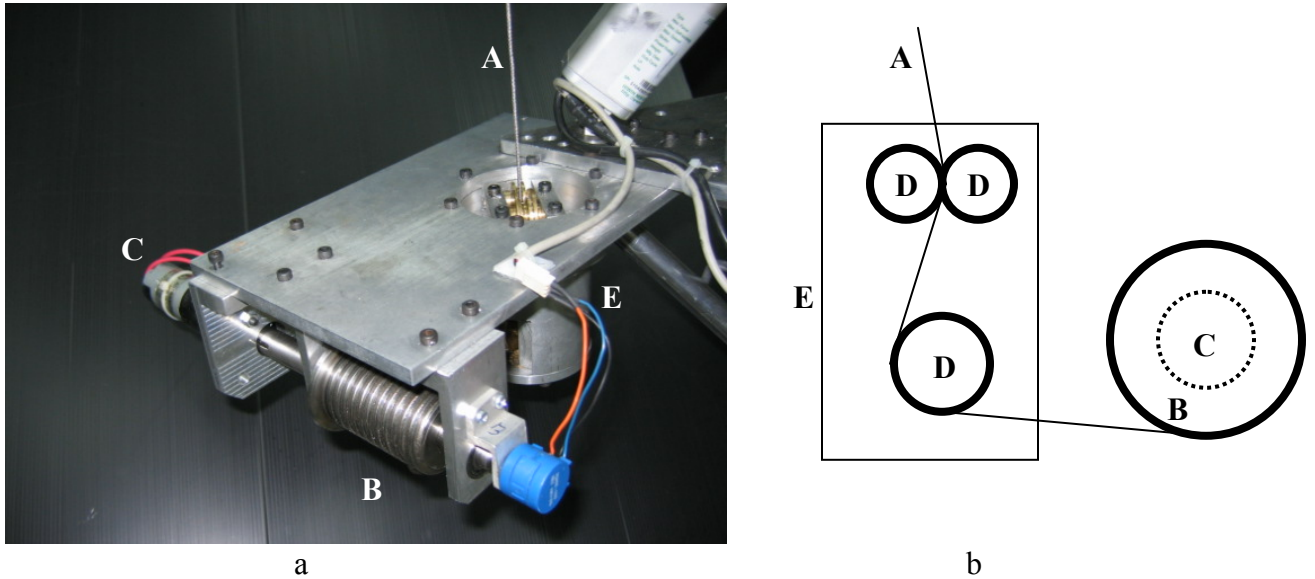
Figure 3.7: Winch – photograph (a) and diagram (b).

There are 3 types of sensors in the mast. Linear potentiometers are mounted on the struts and measure their strokes to calculate their lengths (fig 3.8a).
Rotational potentiometers in the winches are used to measure the rotation of the drum allowing the cables' lengths calculation (fig 3.8b).
Vishay 614 tension compression Load cells are mounted on the cables (fig 3.8a), are used in conjunction with signal amplifiers (fig 3.9) to measure the tension in the cables.

a   b
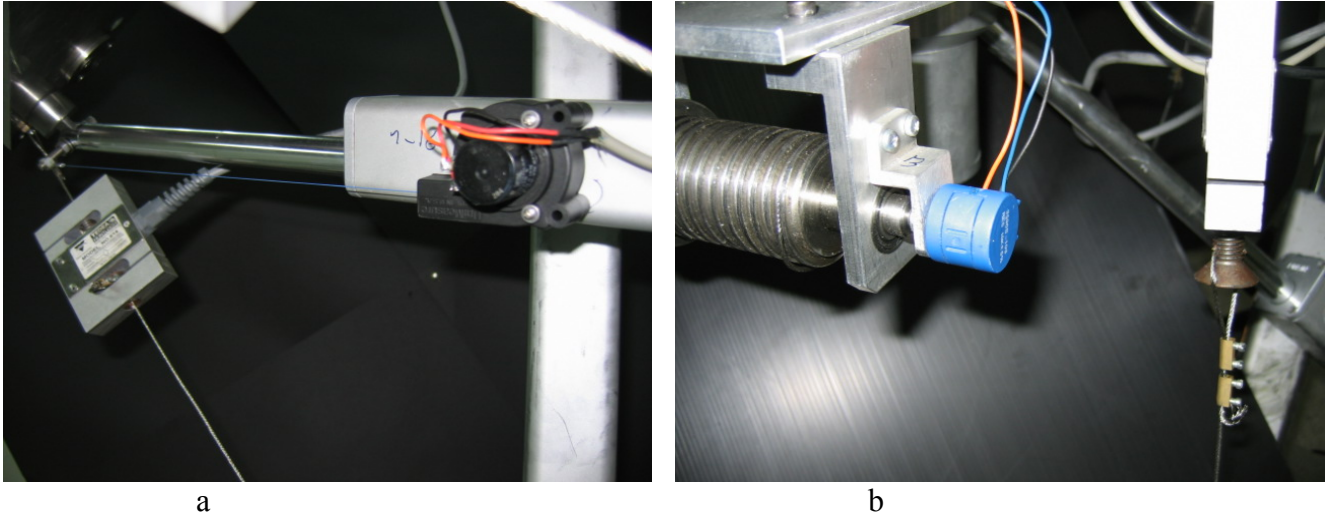
Figure 3.8: Sensors, (a left) load cell (a right) linear potentiometer (b) rotational potentiometer.
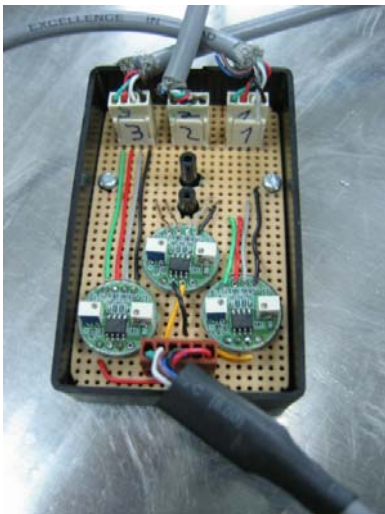
Figure 3.9: Load cell signal amplifiers.

All of the sensors' signals are passed through passive low pass filters to reduce high frequency noise (fig 3.10). The filters use a fixed capacitor (C=10µf) and an adjustable resistor (R=0-10 Kohm) to be able to select a cutoff frequency of 10 Hz.
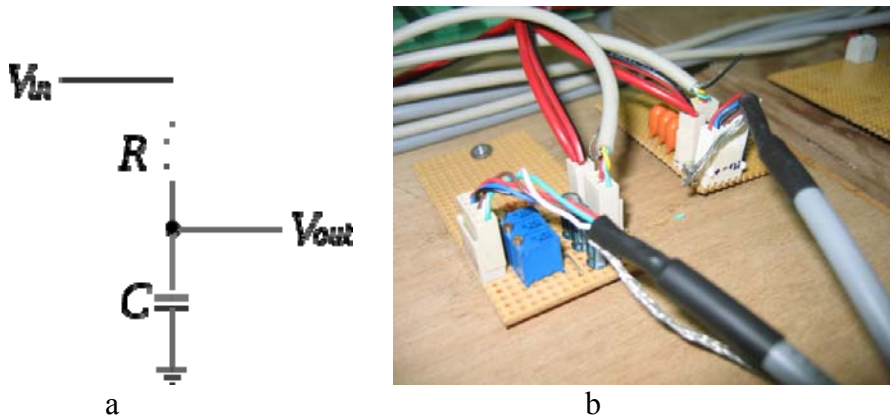
Figure 3.10: Low pass filter (a) circuit diagram (b) two board each with three filters.

Two National Instruments DAQ PCI cards are used to connect the device's sensors and actuators to a PC. The cards used here are NI PCI-6229 and NI PCI-6722 National Instruments DAQ cards. The 2 cards contain 32 single-ended (or 16 differential) analog input channels with 16 bit resolution in the range of ±10V with a sample rate of 250 kS/s, 12 analog output channels with a range of ±10V . Nine A/D channels are used to measure strut lengths, cable lengths and the cable tensions. Six D/A channels supply the control signals to six Advanced Motion Controls Brush Type PWM Servo Amplifiers (fig 3.11 front) driving the struts and winch motors. The amplifiers are needed since the DAQ board cannot supply the voltage and the current required by the actuators. Two 24v power supplies are used, the high current power supply (fig 3.11 rear top) is for the actuators and the low current one (fig 3.11 rear bottom) is for the sensors.
The numbers of channels on the cards and current capacity of the power supply will allow further extension of the device into a 2 staged class 2 mast.
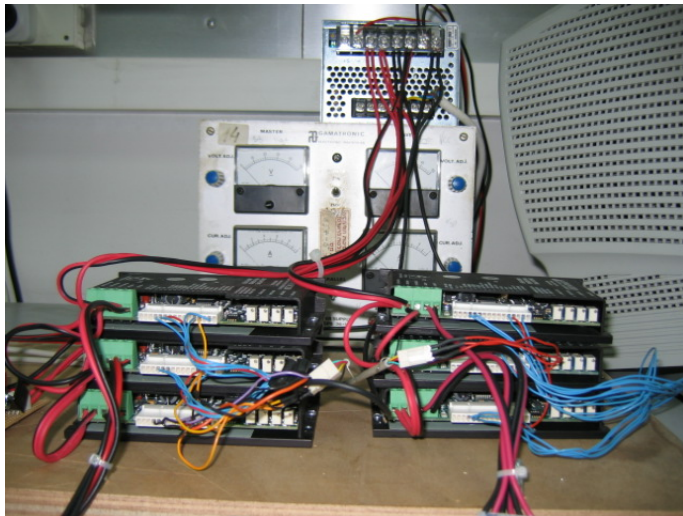
Figure 3.11: Power supplies (back) and power amplifiers (front).

A LabVIEW software package is used to operate the device and to log all of the sensor readings and control outputs to a file for offline analysis of experiment results.
Before the program shuts down, it saves into a log file a table composed of the following columns:

Column number	Data
0	Time stamp (s)
1,2,3	Cable forces (Kgf)
4,5,6	Cable lengths (cm)
7,8,9	Strut lengths (cm)
10,11,12	Top plate accelerations (g)
13,14,5	Cables Setpoints (cm)
16,17,18,	Struts Setpoints (cm)
19,20,21	Cable Control signals (v)
22,23,24	Strut Control signals (v)

The following page shows a flowchart describing the program's algorithm.

```
                        ┌──────────┐
                        │  Start   │
                        └────┬─────┘
                             │
                        ┌────▼─────────┐
                        │ Initialize   │
                        │ input and    │
                        │ output       │
                        │ channels     │
                        └────┬─────────┘
                             │
                        ┌────▼─────────┐
                        │ Read         │
                        │ Positions    │
                        │ and control  │
                        │ parameters   │
                        │ from files   │
                        └────┬─────────┘
                             │
                        ┌────▼─────────┐
                        │ Read current │
                        │ position     │
                        └────┬─────────┘
                             │
                        ┌────▼─────────┐
                        │ Estimate     │
                        │ time         │
                        │ required to  │
                        │ reach next   │
                        │ position     │
                        └────┬─────────┘
                             │
                        ┌────▼─────────┐
                        │ Create       │
                        │ trajectories │
                        │ for position │
                        │ controlled   │
                        │ actuators    │
                        └──────────────┘

  ┌───────────────┐      ┌───────────────┐
  │ Track         │      │ Maintain      │
  │ trajectories  │      │ force with    │
  │ with position │      │ force         │
  │ controlled    │      │ controlled    │
  │ actuators     │      │ actuator      │
  └───────────────┘      └───────────────┘

              ◇ Calcutated time expired? ◇   No
                        │ Yes

              ◇ Final position reached? ◇   No
                        │ Yes

                  ┌──────────────┐
                  │ Stop all     │
                  │ actuators    │
                  └──────────────┘

                  ┌──────────────┐
                  │ Close input  │
                  │ and output   │
                  │ channels     │
                  └──────────────┘

                  ┌──────────────┐
                  │ Write log    │
                  │ data to file │
                  └──────────────┘

                  ┌──────────────┐
                  │     End      │
                  └──────────────┘
```

4. Experiments

4.1. Outline

Experiments were performed using the prototype device to achieve the following objectives: first to validate the proposed shape change algorithm; second to determine the controllers for the actuators that perform adequately regardless of the shape of the device; finally to check the sensitivity of the device to different operating conditions.
In all of the experiments the device was moved through sequence of shapes (Fig 4.1). The sequence has been selected to contain both symmetric and asymmetric shapes, shapes changes which characterize both deployment and retraction and ones that require horizontal translation and angle change of the top platform. These diverse shapes represent the diverse workspace that the device is capable of. The selected shapes were chosen to be in self stress and that there was no contact between the struts.

Table 4.1 Shape change sequence

#	Top plate position	Top plate coordinates (cm) and angles (deg)					Struts and cables lengths (cm)					
		x	y	z	α	β	S1	S2	S3	C1	C2	C3
1	Symmetrical extended	0	0	47	0	0	72	72	72	55.5	55.5	55.5
2	Symmetrical retracted	0	0	22	0	0	57.5	57.5	57.5	33.5	33.5	33.5
1	Symmetrical extended	0	0	47	0	0	72	72	72	55.5	55.5	55.5
3	Translated	10	5	32	0	0	72	67	51	41	49	38
4	Angled	5	0	34	0	30	56	61	68	54	32	38
1	Symmetrical extended	0	0	47	0	0	72	72	72	55.5	55.5	55.5
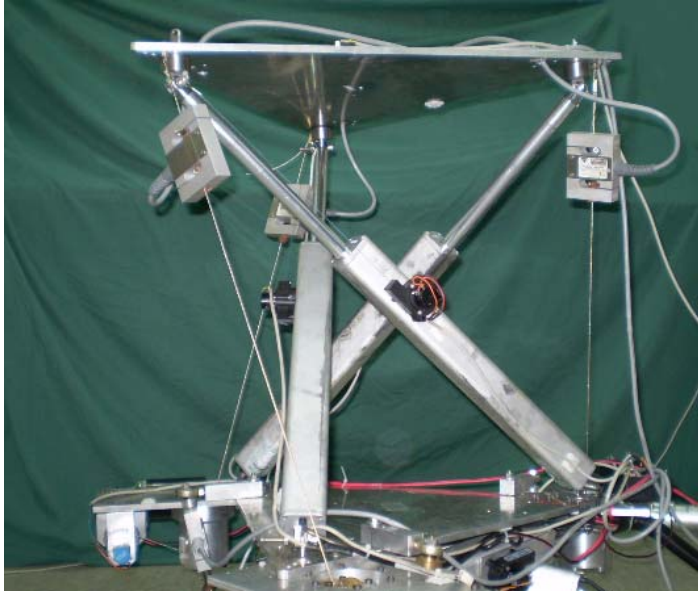
(a)   (b)
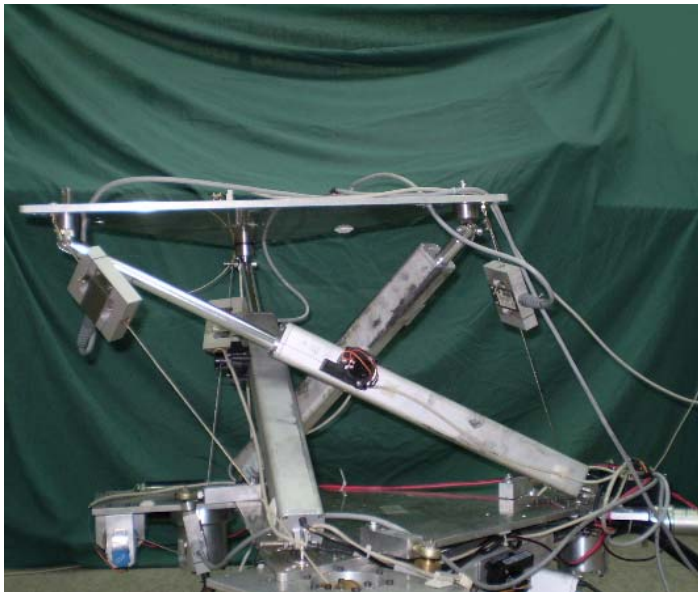
(c)   (d)

Figure 4.1: Top plate position; Symmetrical extended (a), Symmetrical retracted (b), translated (c), angled (d)

4.2. Algorithm validation experiment.

In order to validate the proposed shape change algorithm the device is moved through the shape change sequence. The algorithm should allow the device to change its shape

without loosing its stiffness at any time; therefore the tension in each cable must be positive at all times. The controllers used in this experiment were all the most basic Proportional-Integral-Derivative (PID) controllers (fig 4.2) with only a proportional (P) components and minimal trial and error tuning done to select gains. The selected gains were Kf=1 for the cable force controller, Kcp=1 for the cable position controller and Ksp=10 for the strut position controller.

Figure 4.2: PID controller block diagram.

As the result graphs shows (Fig4.3), the force in each cable was always greater than zero during the shape change sequence which means that the device did not loose its stiffness at any time.
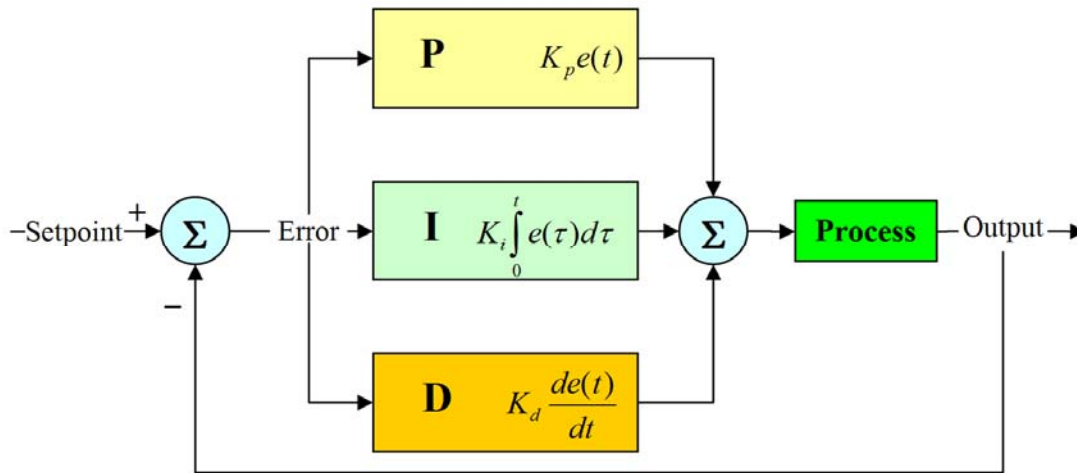
Cable 2

Cable 3

(c)
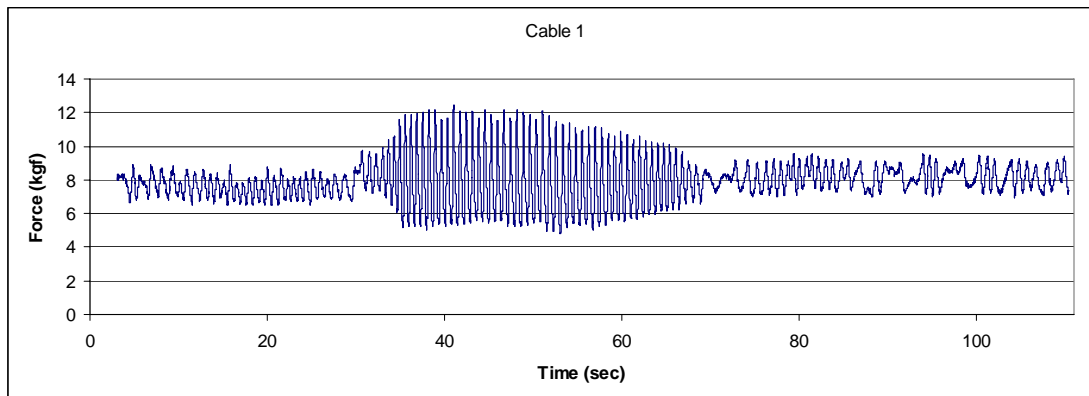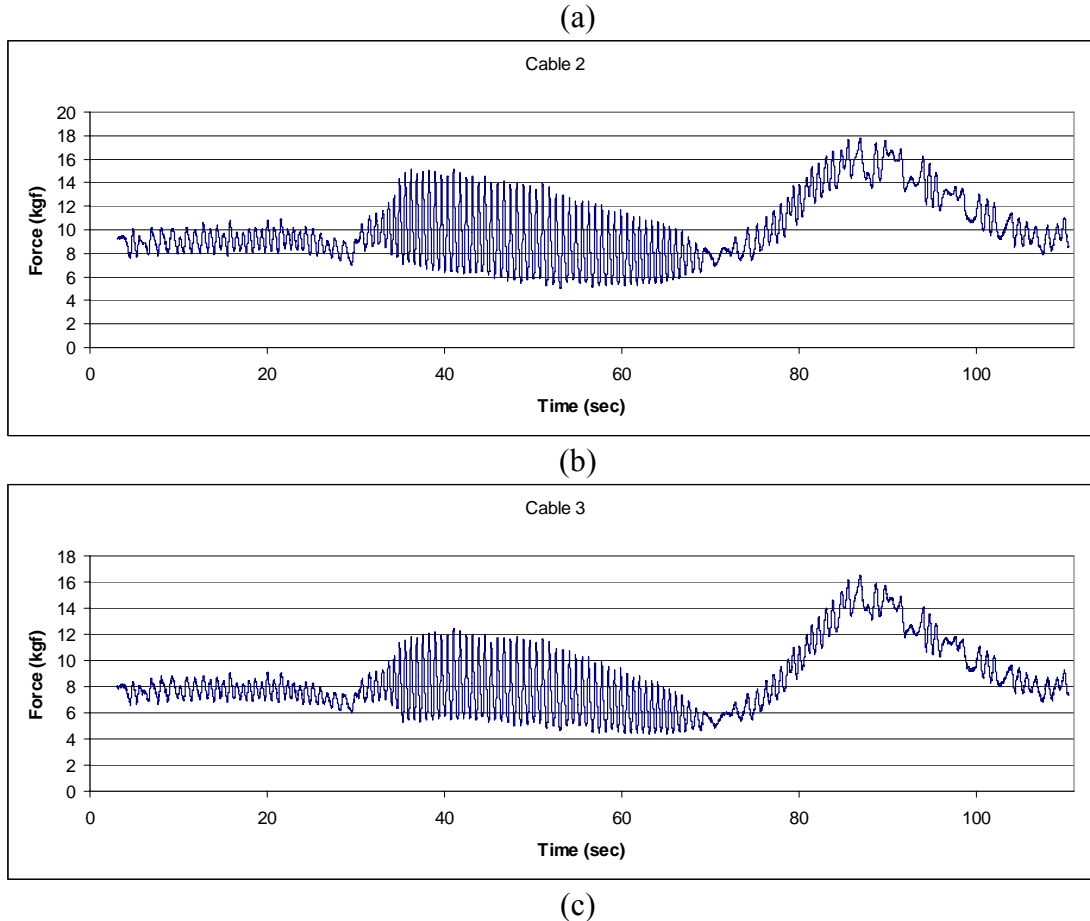
Figure 4.3- Algorithm validation experiment results – forces in force controlled cable (a) and position controlled cables (b,c)

4.3. Controller evaluation experiments.

The first experiment showed that it is possible to change the shape of the device without loosing stiffness by utilizing the proposed algorithm; however, using proportional controllers with minimal gain tuning resulted with a rough and jerky movement with a lot of vibrations as indicated by in the log file. Another issue was the actuators lack in accuracy in tracking their defined trajectories. The object of this series of experiments is to locate controllers and gains for the device that allow for smooth and accurate shape changes.

The device uses three different controllers; a cable force controller for the force controlled cable, a cable position controller for the two position controlled cables and a strut position controller for the three position controlled struts. Each controller was investigated by a separate series of experiments.

4.3.1 Cable force controller evaluation experiments.

The first goal of the cable force controller is to maintain tension in the force controlled cable at all time in order to preserve the rigidity of the device. The second goal is to keep

61

fluctuation in the tension to a minimum. Experiments have shown that there is a correlation between fluctuation in tension cable and visible vibrations in the device. The reason being that large force fluctuation causes the top plate to loose its static equilibrium and the resulting accelerations manifest as vibrations.

The desired tension in the force controlled cable was set to 10 kgf and the effectiveness of each controller was quantified by averaging the absolute values of the tracking errors.

The experiment was composed of a series of runs, in each run the device was moved through the shape change sequence and the average tracking error size recorded. The controller was then changed and a new run conducted. This process was repeated until the average tracking error size could not be significantly reduced.

The first controller that was tested was a constant current controller. Constant current fed to a motor gives constant torque. The experiment showed that constant motor torque did not translate to a constant tension in the cable because some of the torque is used to accelerate the mass of the cable and the top plate. At the acceleration rate required to move the device in the timeframe of the experiments, this controller gave poor results regardless of the current used. The second control tried was a PID controller, at first only with a proportional part and various gains and later with proportional and integral parts and different gains and integration times.

The controller that gave the smallest average tracking error size (0.72 kgf) used a proportional gain of 0.7 and an integration time of 0.02s.

The results of all of the runs are summarized in table 4.2. The cable 1 response graphs of the worst and best run are displayed in figure 4.4.

Table 4.2 Cable force controller experiment results.

Run	Cable force control	Parameters	Average tracking error
1	Constant current	I=0.92 A	66.7%
2	Constant current	I=0.66 A	43.8%
3	Constant current	I=0.53 A	37%
4	Constant current	I=0.37 A	34.5%
5	Proportional	K=0.4	36.4%
6	Proportional	K=0.6	28.9%
7	Proportional	K=0.8	23.9%
8	Proportional	K=1	21.9%
9	Proportional	K=0.7	25.7%
10	Proportional integral	K=0.8 Ti=1	14.3%
11	Proportional integral	K=0.8 Ti=2	12.9%
12	Proportional integral	K=0.8 Ti=0.5	10.7%
13	Proportional integral	K=0.4 Ti=0.3	17.2%
14	Proportional integral	K=0.4 Ti=3	28.8%
15	Proportional integral	K=0.4 Ti=0.05	11.4%
16	Proportional integral	K=0.6 Ti=0.05	8.8%
17	Proportional integral	K=0.8 Ti=0.05	7.7%

18	Proportional integral	K=0.6 Ti=0.04	8%
19	Proportional integral	K=0.6 Ti=0.03	7.8%
20	Proportional integral	K=0.7 Ti=0.03	7.4%
21	Proportional integral	K=0.7 Ti=0.02	7.2%
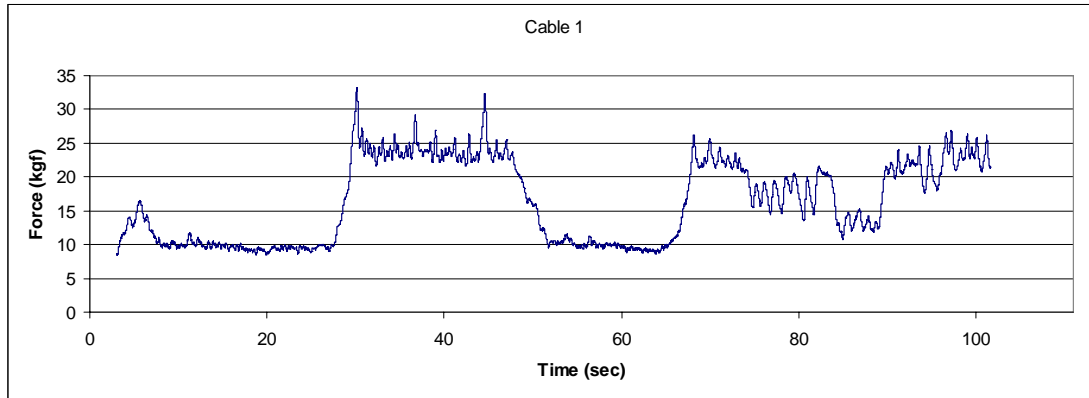
(a)
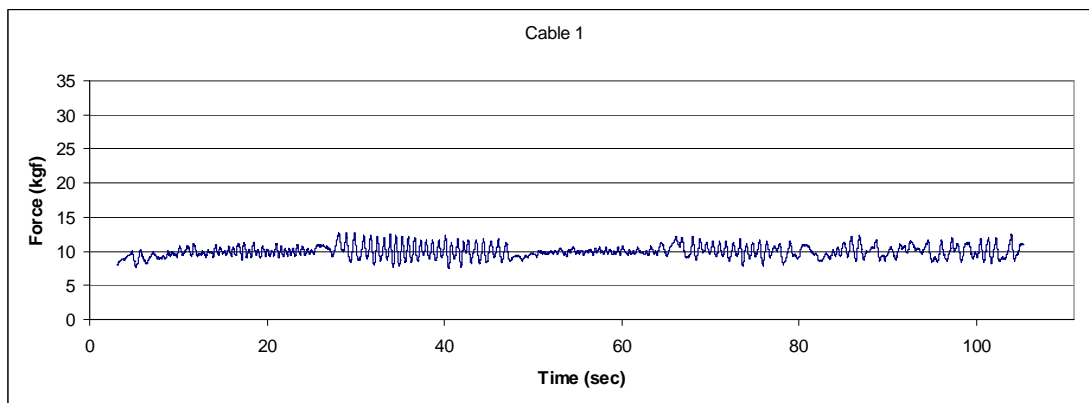
(b)

Figure 4.4: Force in force controlled cable for run 1 (a) and run 21 (b).

4.3.2 Cable position controller evaluation experiments.

The objective of the cable position controller is to follow the length change trajectory assigned to it to allow the device to accurately accomplish the shape change. For each cable a trajectory was calculated to accomplish that all the cables will reach their final length at the same time, while not exceeding the maximum cable velocity starting with a gradual acceleration and ending with gradual deceleration. The effectiveness of the controller was quantified by averaging the absolute values of the tracking errors. An experimental method for adjusting the controllers was used because the lack of a closed system model.

The experiment was composed of a series of runs, in each run the device was moved through the shape change sequence and the average tracking error size recorded. The

force controlled cable's tracking error size (using the same 10 kgf target) was also recorded to make sure improvements in the position control did not come at the expanse of deterioration in the force control. The controller was then changed and a new run conducted. This process was repeated until the average tracking error size could not be significantly reduced.

Various PID controllers were tried, at first only in a proportional configuration and various gains and later with proportional-derivative and proportional-integral configurations and different gains and integration times.
The best controller gave an average tracking error size of 0.1 cm (when the length range was between 32cm and 55.5cm. It used a proportional gain of 1 and an integration time of 0.01s.
The results of all of the runs are summarized in table 4.3. The cable 2 graphs for the trajectory and errors of the worst and best run are displayed in figure 4.5.

Table 4.3: Cable position controller experiment results.

Run	Cable position control	Parameters	Tracking error average size (cm)	Force tracking error
1	Proportional	K=2	0.3	7.7%
2	Proportional	K=3	0.2	8.5%
3	Proportional	K=4	0.16	9.3%
4	Proportional	K=6	0.25	25.8%
5	Proportional	K=5	0.17	17.6%
6	Proportional	K=3.5	0.17	9.5%
7	Proportional	K=4.5	0.15	11.8%
8	PD	Kp=4.5 Kd=0.001	0.17	9%
9	PD	Kp=4.5 Kd=0.0005	0.15	10%
10	PD	Kp=4.5 Kd=0.0001	0.15	10.9%
11	PI	K=4.5 Ti=1	0.14	11.2%
12	PI	K=4.5 Ti=0.1	0.12	11.7%
13	PI	K=3.5 Ti=0.05	0.12	11.8%
14	PD	Kp=3.5 Kd=0.001	0.19	8.3%
15	PI	K=2 Ti=0.05	0.12	7.8%
16	PI	K=1 Ti=0.05	0.19	6.8%
17	PI	K=1.5 Ti=0.05	0.15	7.3%
18	PI	K=1 Ti=0.01	0.10	7.3%
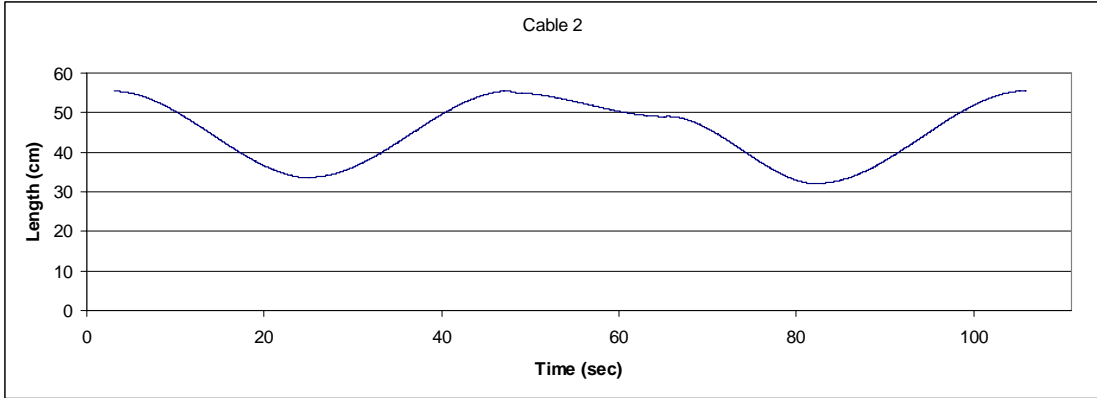
(a)
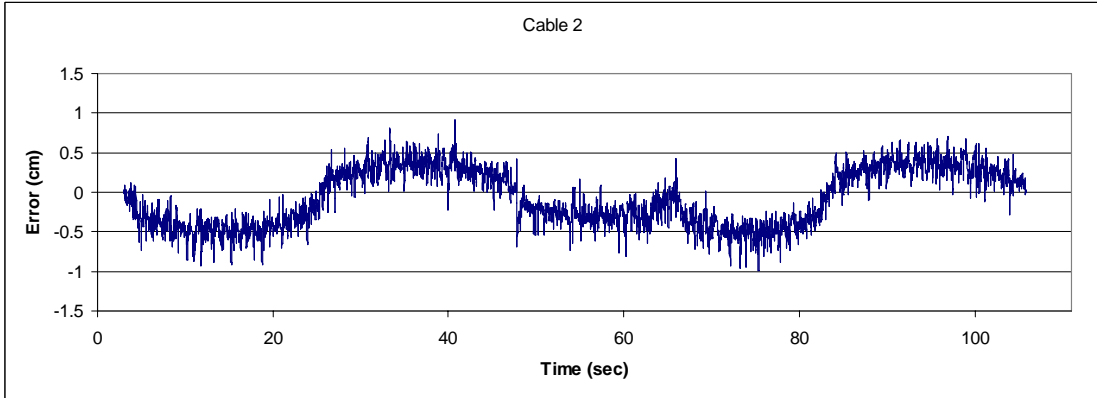
(b)
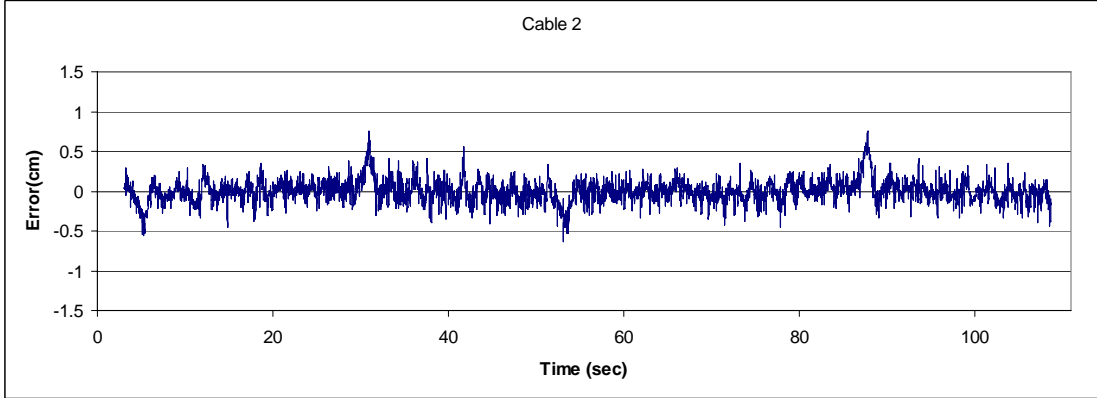
(c)

Figure 4.5: Cable 2 graphs - trajectory (a), run 1 tracking errors (b) and run 18 tracking errors (c).

4.3.3 Strut position controller evaluation experiments.

The objective of the strut position controller is to follow the length change trajectory assigned to it to allow the device to accurately accomplish the shape change (the same principal as for the cable trajectory). The effectiveness of the controller was quantified by averaging the absolute values of the trajectory tracking errors.

The experiment was composed of a series of runs, in each run the device was moved through the shape change sequence and the average tracking error size recorded. The force controlled cable's tracking error size (using the same 10 kgf target) was also recorded to make sure improvements in the position control don't come at the expanse of deterioration in the force control. The controller was then changed and a new run conducted. This process was repeated until the average tracking error size could not be significantly reduced.

Various PID controllers were tried, at first only in a proportional configuration and various gains and later in a proportional-integral configuration and different gains and integration times.
The best controller gave an average tracking error size of 0.12 cm (when the length range was between 56cm and 72cm) without effecting force tracking performance. It used a proportional gain of 18 and an integration time of 5s.
The results of all of the runs are summarized in table 4.4.

Table 4.4: Strut position controller experiment results.

Run	Strut position control	Parameters	Tracking error average size (cm)	Force tracking error
1	Proportional	K=4	0.57	7.3%
2	Proportional	K=6	0.37	7.3%
3	Proportional	K=9	0.25	7.3%
4	Proportional	K=14	0.16	7.3%
5	Proportional	K=21	0.11	8.3%
6	Proportional	K=18	0.12	7.3%
7	Proportional	K=16	0.14	7.9%
8	PI	K=10 Ti=0.1	0.16	7.9%
9	PI	K=10 Ti=1	0.21	7.4%
10	PI	K=18 Ti=5	0.12	7.4%
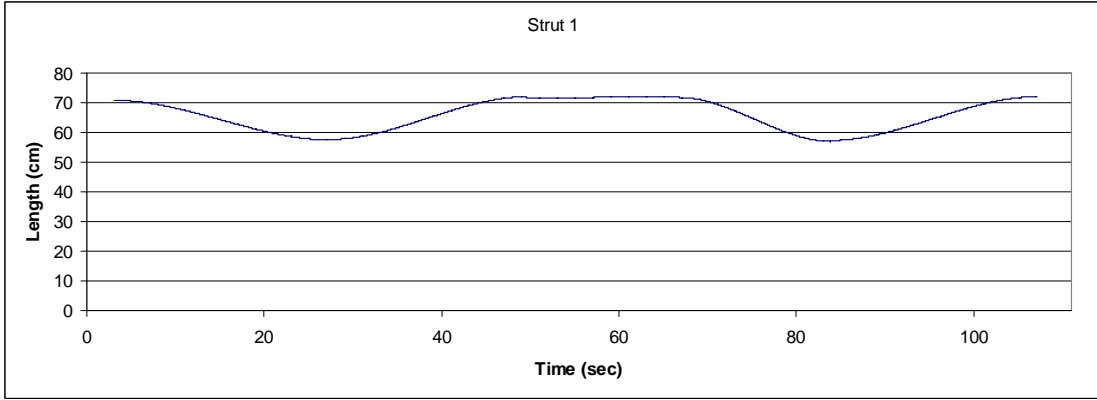
(a)
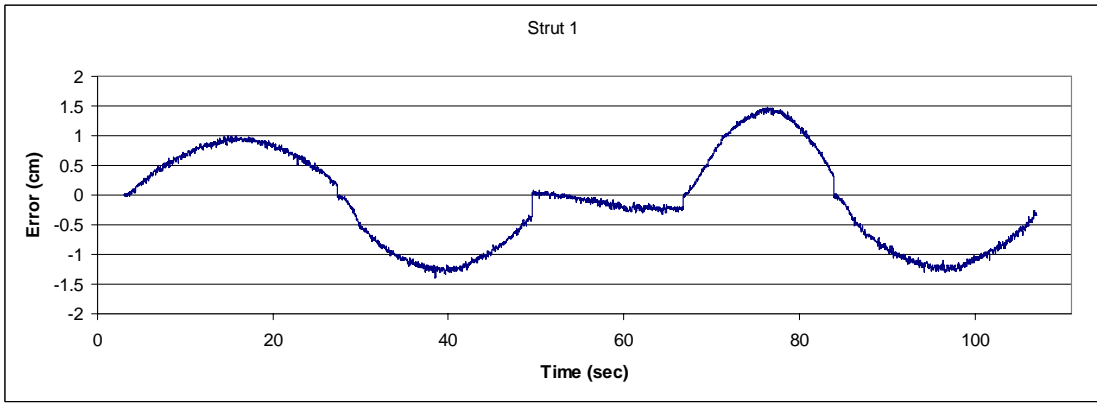
(b)
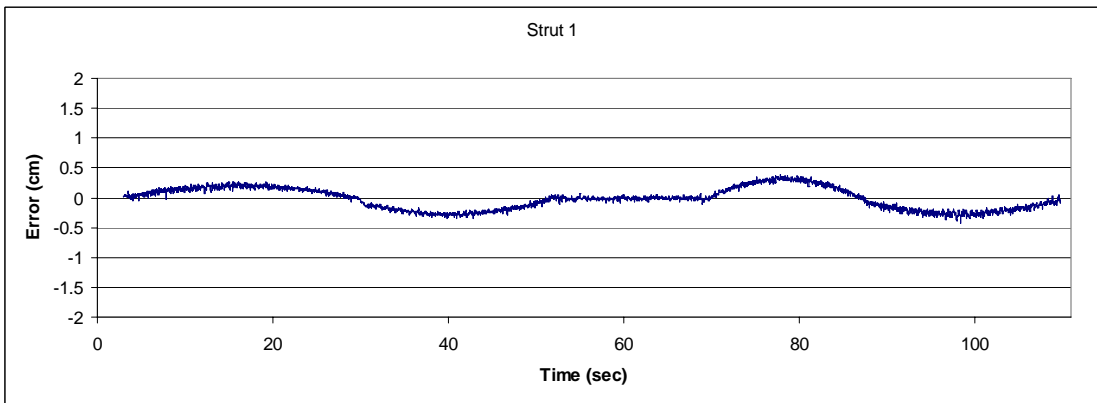
(c)

Figure 4.6: Strut 1 graphs - trajectory (a), run 1 tracking errors (b) and run 10 tracking errors (c).

4.4. Sensitivity evaluation experiments.

After selecting controllers that allow the device to shape change in an accurate manner and with minimal vibrations further experiments were performed to determine the effect of changing conditions on the performance of the device.

All experiment was composed of a series of runs; in each run the device was moved through the shape change sequence the all average tracking error sizes recorded to measure the effect on the performance of the device. The parameter was then changed and a new run conducted several times.

Three parameters were varied in the course of the experiments load, pre-stress and speed. The controllers were calibrated in the previous experiments with no load, 10 kgf pre-stress and maximal speed.

Loads
Concrete blocks of different weights of up to 7 kg have been attached to the top platform to create a load. The device showed a small deterioration in performance with the increased load as seen in table 4.5.

Table 4.6: Load experiment results.

Run	Load (kg)	Strut tracking error average size (cm)	Cable tracking error average size (cm)	Force tracking error
1	0	0.12	0.1	7.2%
2	1.5	0.12	0.1	8%
3	5.5	0.12	0.1	7.5%
4	7	0.12	0.1	7.5%

Pre-stress
The force controlled cable's was set to a different pre-stress target between 7.5 kgf and 15 kgf for each run. As the set pre-stress level was increased, the device showed an improvement in force tracking with a small worsening in strut position tracking, as seen in table 4.7.

Table 4.7: Pre-stress experiment results.

Run	Pre-stress (kgf)	Strut tracking error average size (cm)	Cable tracking error average size (cm)	Force tracking error
1	7.5	0.12	0.1	8.4%
2	10	0.12	0.1	7.2%
3	12.5	0.13	0.1	7.2%
4	15	0.13	0.1	6.6%

Speed

The maximal shape changing speed of the device is limited by the struts' maximal length change rate of 10 mm/sec. The trajectories for each run have been set using different strut length change rate to achieve different shape change speed. The device showed improvement in performance with speed reduction as seen in Table 4.8.

Table 4.8: Speed experiment results.

Run	Speed	Strut tracking error average size (cm)	Cable tracking error average size (cm)	Force tracking error
1	100%	0.12	0.1	7.2%
2	75%	0.1	0.09	7.1%
3	50%	0.07	0.08	6.7%

Examination of the sensitivity experiments' results shows that the force tracking has some sensitivity to changing condition with a swing of 0.32 kgf between the best and worst cases tested, while the position tracking was almost insensitive with a swing of only 0.06 cm between the best and worst cases tested.

5. Conclusions

This work introduces a new approach for the shape change process of tensegrity structures. This approach allows each actuator to be controlled individually as opposed to the common approach that requires coordinated control of all actuators. It is based on the topological properties of the structure and requires minimal time and processing power.

The approach has been proven both theoretically and experimentally to allow the shape change of a tensegrity device based on the topology of a T-3 tensegrity prism. It is also applicable to any topology which is an Assur Graph.

The shape change process of the tensegrity device proved to be flexible and robust, i.e., it maintained a good level of performance regardless of the operation requirements such as target position, load, pre-stress and speed.

An area to explore is the behavior of devices with more degrees of freedom. The additional degrees of freedom can come either from using the same topology with more actuated members, two or more instances of the current topology connected in series or from a different and more complex topology.
At this time research is underway to develop a caterpillar-like tensegrity device composed of multiple Triad stages (Figure 5.1)
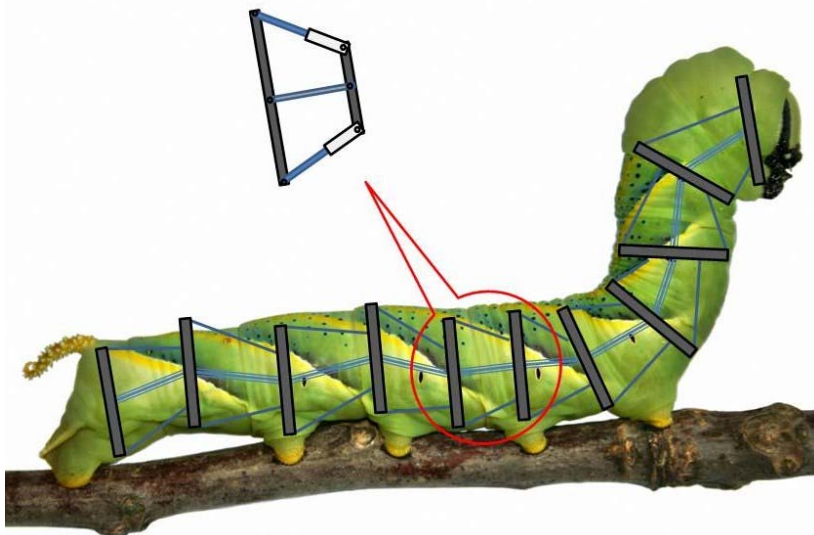

Figure 5.1 – Multiple Triad device proposal.

Another direction being considered is tensegrity devices with the ability to change not only their geometry but also their topology, changing it from one Assur Graph to another.

6. Bibliography

Artobolevskii, I. I. Teoriya mehanizmov i masin. Gosudarstv. Izdat. Tehn.-
Teor., Moscow-Leningrad, 2d ed., 1951.

Assur, L. V., Issledovanie ploskih sterznevyh mehanizmovs nizsimi paramis tocki
zreniya ih struktury i klassifikacii, Izdat. Akad. Nauk SSSR, 1952.

Ben-Horin, P. and Shoham, M., "Singularity analysis of a class of parallel robots based
on Grassmann-Cayley algebra", *Mech. Mach. Theory*, vol. 41, pp. 958-970, 2006

Fest, E., Shea, K., Domer, B. and Smith, I. F. C.. "Adjustable
tensegrity structures*.", J. Struct. Eng*., vol. 129, pp. 515–526, 2003.

Fest E., Shea K., and Smith I. F. C., "Active Tensegrity Structure", *J. Struct. Eng*, vol.
130, pp. 1454, 2004.

Fuller, R. B. Tensile-integrity structures. United States Patent 3,063,521,
1962. Filed 31 August 1959, Granted 13 November 1962.

Gantes, C.J, "Deployable Structures – Analysis and Design", WIT Press, Southampton,
England, 2001.

Kanchanasaratool N., Williamson D., "Motion control of a tensegrity platform"
Communications in Information and Systems, vol. 2, no. 3, pp. 299-324, December 2002

Masic, M. and Skelton, R. E. , "Open–loop control of class–2 tensegrity towers," in
Proceedings of SPIE's 11th Annual International Symposium on Smart Structures and
Materials, San Diego, CA, USA, March 2004.

Pinaud, J. P., Masic M. and Skelton, R. E.. "Path Planning for the Deployment of
Tensegrity Structures". In Proceedings of the SPIE Smart Structures and Materials:
Modeling, Signal Processing, and Control, vol. 5049, pp. 436–447, San Diego, San
Diego, CA, USA, March 2003.

Pinaud, J. P., Solari, S. and Skelton, R. E.. "Deployment of a Class 2 Tensegrity Boom".
In Proceeings of the SPIE Smart Structures and Materials: Smart Structures and
Integrated Systems, vol. 5390, pp. 155–162, San Diego, CA, USA, March 2004.

Parker S. P., "McGraw-Hill dictionary of scientific and technical terms" 5th ed.,
McGraw-Hill, 1994.

Paul, C., Lipson, H., and Valero-Cuevas, F.J. "Gait Production in a Tensegrity Based Robot". In Proc. Int. Conf. on Advanced Robotics, Seattle, WA, USA, July 2005a.

Paul, C. Lipson, H. and Valero-Cuevas, F.J. "Redundancy in the Control of Robots with Highly Coupled Mechanical Structures", Int. Conf. on Intelligent Robots and Systems, pp. 802-808, Edmonton, Canada, August 2005b

Paul, C., Valero-Cuevas, F.J and Lipson, H. " Design and control of tensegrity robots for locomotion ". In IEEE transactions on robotics, vol. 22, no. 5, October 2006

Servatius B., Shai O. and Whiteley W., Geometric Properties of Assur Graphs, accepted for publication in the *European Journal of Combinatoric*, 2009.

Shai O., "The Canonical Form of All Planar Linkage topologies", ASME Design Engineering Technical Conferences, in San Diego, California, USA, August 30 – September 2, 2009.

Shai, O. and Polansky,I., "Finding Dead-Point Positions of Planar Pin-Connected Linkages Through Graph Theoretical Duality Principle", *J. Mech. Des*. 128, 599, 2006

Skelton, R. E. Adhikari, R. Pinaud, J. Chan and W. Helton, J. W. "An introduction to the mechanics of tensegrity structures" Proceedings of the IEEE Conference on Decision and Control. Vol. 5, pp. 4254-4259, 2001.

Soong T.T. and Manolis G.D., "Active structures", *J. Struct. Eng.* Vol. 113, No. 11, pp. 2290-2302, November 1987

Sultan C., Corless M. and Skelton, R. E., "Tensegrity flight simulator," *J. Guid., Control, Dyn.*, vol. 23, no. 3, pp. 1055–1064, 2000.

Sultan C., Corless M.and Skelton, R.E., "The prestressability Problem of Tensegrity structures: some analytical solutions", *International Journal of Solids and Structures*, vol.38, pp. 5223-5252, July 2001.

Sultan, C. and Skelton, R. "Deployment of tensegrity structures". *International Journal of Solids and Structures*, vol. 40, pp. 4637-4657, 2003

van de Wijdeven J. and, de Jager B. "Shape Change of Tensegrity Structures: Design and Control", 2005 American Control Conference, June 2005.

Whittier, W.B., "Kinematic Analysis of Tensegrity Structures", Masters Thesis, Virginia Polytechnic Institute & State University, November 2002.

Williamson, D., Skelton R.E. and Han J., "Equilibrium conditions of a Tensegrity structure", *International Journal of Solids and Structures*, vol. 40, pp. 6347–6367, 2003

תקציר

מתקני טנזגריטי הם מבנים מיוחדים דמויי מסבך המורכבים ממוטות הנתונים במאמצי לחיצה וכבלים הנתונים במאמצי מתיחה. מתקן טנזגריטי יהיה קשיח כאשר על כל מרכיביו יופעל מאמץ. מתקן טנזגריטי מסוגל לשנות את הגאומטריה שלו בעזרת שימוש במפעילים המשנים את אורכי המוטות והכבלים. בגלל יכולת זו, מתקני טנזגריטי מתאימים לשמש כבסיס למבנים נפרשים, מבנים חכמים ורובוטים.

שינוי הגאומטריה של מתקני טנזגריטי כולל שני שלבים חשובים. שלב ראשון הוא מציאת הצורה (זיהוי הגיאומטריות בהן על כל מרכיבי המתקן פועל מאמץ). השלב השני הוא שינוי הצורה (המעבר בין שתי גאומטריות אפשריות ללא אובדן קשיחות המתקן). השיטות הידועות כיום מבוססות על תהליכים הדושים כח מחשוב וזמן רבים כמו סימולציות ואופטימיזציות בקנה מידה גדול.

עבודה זו מציגה אסטרטגית שינוי צורה חדשה המבוססת על התכונות המיוחדות של מבני אסור. מבני אסור (Assur Graphs) הידועים מזה זמן רב בתחום הקינמטיקה נחקרו בתקופה האחרונה על ידי מתמטיקאים העוסקים בתאוריית הקשיחות שפיתחו משפתים ואלגוריתמים חדשים בתחום. האסטרטגיה החדשה הינה מהירה ואינה דורשת כח מחשוב רב. ניתן להפעיל את האסטרטגיה על כל מתקן שהטופולוגיה שלו היא אחת מאינסוף גרפי אסור.

אלגוריתם שינוי הצורה שפותח מאפשר למתקן לעבור מצורה לצורה מבלי לאבד את קשיחותו. שינוי הצורה מבוצע על ידי שינוי אורכי האלמנטים של המבנה. בעזרת האלגוריתם חלק מן האלמנטים משנים את אורכם בצורה שרירותית כדי להגיע לצורה הסופית, בזמן שאלמט אחד בלבד נשלט בצורה שתבטיח את קשיחות המתקן.

השיטה פותחה ונבדקה בעזרת אב טיפוס של מתקן טנזגריטי שתוכנן ונבנה למטרת ביצוע ניסויים. ניסויים באב הטיפוס הראו שהשיטה החדשה מאפשרת למתקן לשנות את צורתו.

אוניברסיטת תל - אביב
הפקולטה להנדסה ע״ש איבי ואלדר פליישמן
בית הספר לתארים מתקדמים ע״ש זנדמן-סליינר

אלגוריתם לשינוי צורה של מתקן טנזגרטי

חיבור זה הוגש כעבודת גמר לקראת התואר ״מוסמך אוניברסיטה״ בהנדסה מכנית

על - ידי

אבנר ברונפלד

העבודה נעשתה במחלקה למכניקה, חומרים ומערכות בהנחיית
דר׳ אורי בן-חנן
דר׳ עופר שי

הדר תשס״ע

`

אוניברסיטת תל - אביב

אוניברסיטת תל - אביב
הפקולטה להנדסה ע"ש איבי ואלדר פליישמן
בית הספר לתארים מתקדמים ע"ש זנדמן-סליינר

אלגוריתם לשינוי צורה של מתקן טנזגרטי

חיבור זה הוגש כעבודת גמר לקראת התואר "מוסמך אוניברסיטה" בהנדסה מכנית

על - ידי

אבנר ברונפלד

`